Role of *Arabidopsis thaliana* RING-Type E3 Ligase XBAT35.2 in Regulating ACD11 Stability

by

Sarah McVey

Submitted in partial fulfillment of the requirements
for the degree of Master of Science

at

Dalhousie University
Halifax, Nova Scotia
June 2015

I dedicate this work to my parents, with love.

Table of Contents

List of Tables

List of Figures

Abstract

Ubiquitination is a post-translational modification that results in a single (monoubiquitination) or multiple (polyubiquitination) ubiquitin molecule(s) being covalently attached to a selected protein substrate. A common consequence of ubiquitination is degradation of the polyubiquitinated protein by the 26S proteasome. Ubiquitination requires the sequential action of three enzymes: E1 (ubiquitin activating enzyme), E2 (ubiquitin conjugating enzyme), and E3 (ubiquitin ligase). E1 activates ubiquitin and E2 receives the activated ubiquitin from E1. The E2-ubiquitin intermediate interacts with the E3, which recruits the substrate. The E2 and E3 then coordinate the attachment of ubiquitin to a lysine residue on the selected protein substrate. My research focuses on characterizing the function of the RING-type E3 ligase, XBAT35.2, via identification of substrates for the E3 ligase. Accelerated Cell Death 11 (ACD11) has been identified as a potential substrate for XBAT35.2. ACD11 is a pathogen-related protein that is an important component of the programmed cell death pathway in plants. *acd11*, a lethal recessive mutant in Arabidopsis, constitutively expresses cell death and defense related genes. ACD11 is thought to inhibit cell death and activation of defense pathways in the absence of pathogens. The interaction between ACD11 and XBAT35.2 was confirmed using immunoprecipitation assays. Cell free degradation assays were used to determine if ACD11 was a target for the ubiquitin proteasome system and also to demonstrate that XBAT35.2 mediated the turnover of ACD11. My results show that ACD11 is quite stable in a cell free degradation assay, however, when transiently co-expressed with XBAT35.2, ACD11 is rapidly turned over. I also demonstrate that XBAT35.2-mediated turnover of ACD11 is dependent on the function of the 26S proteasome. Unexpectedly, XBAT35.2 is itself unstable and subjected to proteasome dependent degradation. The observed turnover of XBAT35.2 requires its own RING E3 ligase activity as the nonfunctional E3 is not degraded. This suggests that XBAT35.2 undergoes self-ubiquitination and auto-regulation. These results provide evidence that ACD11 is a substrate for XBAT35.2 E3 ligase activity. These results also correlate with previous studies, which show that overexpression of XBAT35.2 is capable of inducing cell death in tobacco cells and promoting plant defense against pathogens in Arabidopsis transgenic plants. A model is proposed where in the absence of pathogen, XBAT35.2 is continually self-ubiquitinated and degraded by the 26S proteasome, allowing ACD11 to accumulate and inhibit cell death and pathogen defense pathways. In the presence of pathogens, XBAT35.2 would be stable and promote the degradation of ACD11, allowing for activation of cell death and defense response pathways.

List of Abbreviations Used

ABRC	Arabidopsis Biological Resource Center
ACD11	Accelerated Cell Death 11
ANK	Ankyrin
Asp	Aspartic acid
ATP	Adenosine triphosphate
AtPRA1	*Arabidopsis thaliana* Prenylated Rab acceptor 1
BAK1	Brassinosteroid insensitive 1-associated kinase 1
BiFC	Bimolecular fluorescence complementation assay
BRCA1	Breast cancer 1, early onset
BRCT	BRCA1 C terminus
C1P	Ceramide-1-phosphate
cDNA	Complementary DNA
Cer	Ceramide
CRL	Cullin RING ligase
CRL1	Cullin RING ligase 1
CUL1	Cullin 1
DNA	Deoxyribonucleic acid
DUB	Deubiquitinating enzyme
E1	Ubiquitin-activating enzyme
E2	Ubiquitin-conjugating enzyme
E3	Ubiquitin ligase
ECL	Enhanced Chemiluminescence

EDTA	Ethylenediaminetetraacetic acid
EGTA	Ethylene glycol tetraacetic acid
FLS2	Flagellin-sensitive 2
GFP	Green fluorescent protein
GLTP	Glycolipid transfer protein
Glu	Glutamic acid
HA	Hemagglutinin
HECT	Homologous to E6-AP carboxyl terminus
HEPES	4-(2-hydroxyethyl)-1-piperazineethanesulfonic acid
HERC	Domain homologous to E6 associated protein carboxy-terminus and RCC1 domain protein
IP	Immunoprecipitation
kD	Kilo dalton
LCB	Long-chain bases
Lys	Lysine
MDa	Mega Daltons
MES	2-(N-morpholino) ethane sulfonic acid
MG132	N-(benzyloxycarbonyl)leucinylleucinylleucinal Z-Leu-Leu-Leu-al
mM	Millimolar
NLS	Nuclear localization signal
OD	Optical density
PCD	Programmed Cell Death
PR1/PR2	Pathogenesis-related genes

PRR	Pattern-recognition receptor
Pst DC3000	*Pseudomonas syringae* pv. *tomato* 3000
PUB	Plant U-Box
PVDF	Polyvinylidene fluoride
Rbx	RING box protein 1
RING	Really interesting new gene
RT-PCR	Reverse transcription polymerase chain reaction
S1P	Sphingosine 1-phosphate
SCF	Skp1, Cullins, F-box proteins
Skp1	S-phase kinase-associated protein 1
SDS	Sodium dodecyl sulfate
SDS-PAGE	Sodium dodecyl sulfate polyacrylamide gel
TBS	Tris-buffered saline
TBST	Tris-buffered saline and Tween 20
U-box	UFD2-homology domain
UPS	Ubiquitin Proteasome System
WB	Western blot
WD40	Trp-Asp 40
XB3	XA21-binding protein 3
XBAT	XB3 ortholog in *Arabidopsis thaliana*
YC	YFP carboxyl-terminus
YFP	Yellow fluorescent protein
YN	YFP amino-terminus

Acknowledgements

A special thanks to my supervisor, Dr. Sophia Stone, for your incredible guidance and patience over the last two years. I have learned an immense amount of knowledge from you, and I am looking forward to applying those skills to my future endeavors.

Thank you to Dr. Bill Pohajdak and Dr. Patrice Côté for being on my committee and for providing helpful suggestions along the way.

I would like to thank my parents and my siblings for their unconditional love and support throughout this challenging journey.

Thank you to my fellow lab mates Daryl McNeilly and Victoria Sullivan for making my workdays so enjoyable. Your advice on laboratory techniques was extremely appreciated. Special thanks to our PhD student Wendy Lyzenga for her knowledgeable wisdom and motivating talks.

Chapter 1: Introduction

1.1) Ubiquitin Proteasome System (UPS)

The ubiquitin proteasome system (UPS) plays a crucial role in the majority of plant growth and developmental processes. The system involves two successive and distinct steps: 1) the selection and ubiquitination of a substrate protein and 2) the degradation of the modified protein by the 26S proteasome. The UPS is a highly conserved regulatory network that plays an important role in cellular housekeeping functions that are essential for proper growth and development in all eukaryotes (Craig, Ewan, Mesmar, Gudipati & Sadanandom, 2009; Smalle & Vierstra, 2004). A large portion of the *Arabidopsis thaliana* (Arabidopsis) proteome is dedicated to the UPS. For example, the genes that encode for the ubiquitin enzymes accounts for over 5% of the Arabidopsis genome (Smalle & Vierstra, 2004). Proteasomal degradation of misfolded proteins and the removal of rate-limiting enzymes are key regulatory components of the UPS that enable eukaryotes to maintain homeostasis (Craig et al., 2009). The UPS is also involved in numerous cellular processes including transcriptional regulation, cell cycle progression, and cellular responses to abiotic and biotic stresses (Smalle & Vierstra, 2004). Specific substrates that are regulated by ubiquitin-dependent protein degradation include abnormal proteins, structural proteins, enzymes, nuclear transcription activators and repressors, and other short-lived regulatory proteins (Glickman & Ciechanover, 2002; Stone et al., 2005).

Ubiquitination

Ubiquitination is a post-translational modification that results in ubiquitin

molecule(s) being covalently attached to an internal lysine of a selected protein substrate (Sun & Chen, 2004; Vierstra, 2009). Ubiquitin is a 8.5kD molecule comprised of 76 amino acids (Callie et al., 1995). All eukaryotic organisms contain ubiquitin and it is expressed in all tissue types. This globular protein has a conserved gene sequence, with only three amino acids differing between human species and yeast species (Callis et al., 1995; Craig et al., 2009). Ubiquitin contains intramolecular hydrogen bonds, which stabilize ubiquitin and make recycling a more common fate for the molecule, as proteolysis is more energetically expensive (Craig et al., 2009). Ubiquitin is also inherently heat stable, as the density of hydrophobic side chains is high in the ubiquitin core and prevents denaturation (Lenkinsiki et al., 1977; Khorasanizadeh, Peters, Butt & Roder, 1993). A single (monoubiquitination) or multiple (polyubiquitination) ubiquitin molecule(s) in the form of a chain can be attached to a substrate. Multi-monoubiquitination can also occur, which is the attachment of multiple ubiquitin molecules on a recruited substrate without forming a continuous polyubiquitin chain (Haglund et al., 2003).

Ubiquitination requires the sequential action of three enzymes: ubiquitin-activating enzymes (E1s), ubiquitin-conjugating enzymes (E2s), and ubiquitin ligases (E3s) (Smalle & Vierstra, 2004) (Figure 1). The Arabidopsis genome consists of approximately two isoforms for E1, 47 E2s, and more than 1400 E3s (Smalle & Vierstra, 2004). In the first step of the ubiquitination pathway, the E1 activates ubiquitin in an ATP-dependent reaction, forming a thioester linked intermediate (Stone, Hauksdottir, Troy, Herschleb, Kraft, & Callis, 2005). The E2 then receives the activated ubiquitin from the E1, also forming a thioester linked E2-ubiquitin intermediate. The E2-ubiquitin

intermediate interacts with E3 ubiquitin ligase, which recruits a specific substrate and subsequently mediates the attachment of ubiquitin to a lysine residue on the selected protein substrate (Glickman & Ciechanover, 2002) (Figure 1). The conjugation process is repeated to build a polyubiquitin chain via ubiquitin-ubiquitin linkages. Monoubiquitination is involved in repair of damaged DNA, receptor endocytosis, and regulation of histone function (Haglund, Fiore, & Dikic, 2003; Hicke, 2001) (Figure 1). Multi-monoubiquitination is a modification also commonly involved in receptor endocytosis (Haglund et al., 2003). In addition to the number of ubiquitin molecules attached to the substrate, linkage characteristics in a ubiquitin chain play a role in determining the fate of ubiquitinated proteins (Weissman, 2001; Stone et al., 2005). Specifically, the type of internal lysine residue used in the formation of ubiquitin-ubiquitin linkages within the chain can determine the outcome of polyubiquitination. Seven lysine residues located at positions 6, 11, 27, 29, 33, 48, and 63 on a ubiquitin molecule can be used in the formation of a polyubiquitin chain (Peng et al., 2003) (Figure 1). Lysine-63 linked chains, for example, are involved in protein kinase activation and endocytosis (Passmore & Barford, 2004), whereas degradation by the 26S proteasome requires a lysine-48 linked chain (Stone et al., 2005; Deng et al., 2000). The attachment of a polyubiquitin chain containing at least four lysine-48 linked ubiquitin molecules is required for degradation by the 26S proteasome (Glickman & Ciechanover, 2002).

The 26S Proteasome

The 26S proteasome is a 2.5 megadalton (MDa) structure composed of approximately 31 different subunits. The structure of the 26S proteasome consists of two

Figure 1. Ubiquitination Pathway. E1 (ubiquitin-activating enzyme) activates a ubiquitin molecule, which is then transferred to the E2 (ubiquitin-conjugating enzyme) in the initial steps. The E2-ubiquitin intermediate then interacts with E3 (ubiquitin ligase enzyme). Ubiquitin is then transferred to lysine residues on a specific substrate bound to the E3. The process is repeated to build a polyubiquitin chain.

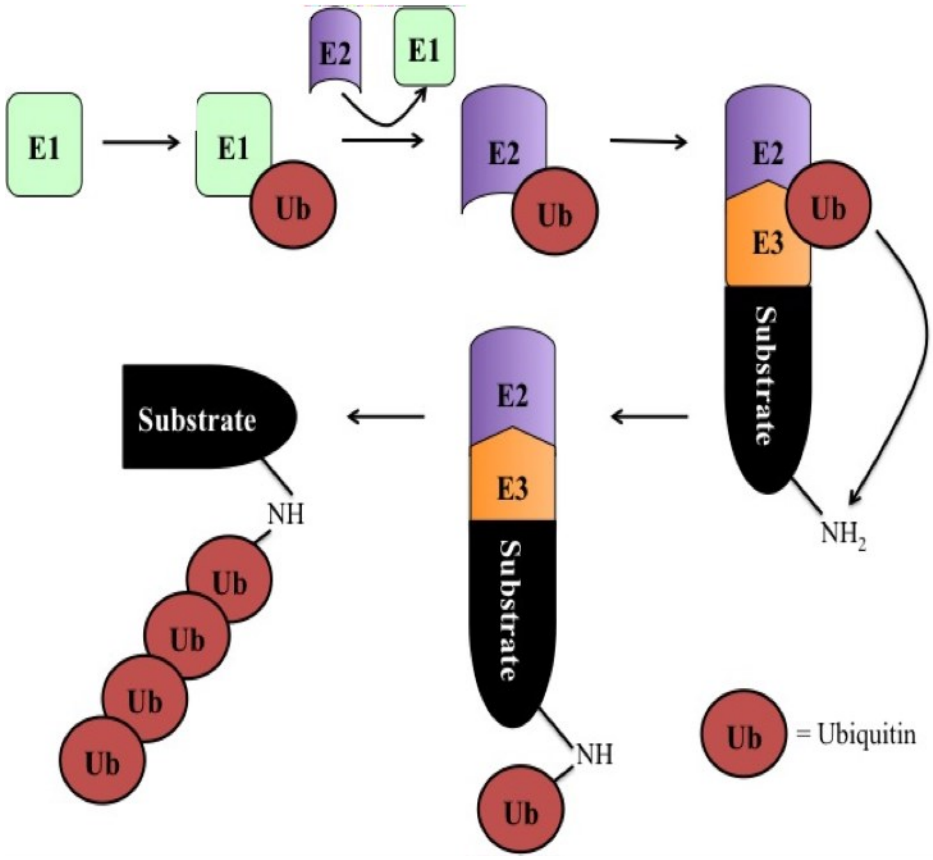
E1
E1
Ub
E2
E1
E2
Ub
E2
E3
Ub
Substrate
NH2
E2
E3
Substrate
NH
Ub
Substrate
NH
Ub
Ub
Ub
Ub
Ub = Ubiquitin

19S regulatory caps at each end of a core 20S proteasome complex (Figure 2).

Once a selected protein substrate has been polyubiquitinated with at least four lysine-48 linked ubiquitin molecules, the modified protein is targeted to the 26S proteasome for degradation. The polyubiquitinated protein is first recognized and bound by the 19S regulatory cap, which is also subsequently responsible for unfolding and translocating the targeted protein into the 20S core complex (Lecker, Goldberg, & Mitch, 2006). The polyubiquitin chain is cleaved from the substrate and disassembled by deubiquitinating enzymes (DUBs) in the 19S regulatory cap so that the ubiquitin molecules can be recycled and reused in the UPS pathway (Lecker et al., 2006; Voges et al., 1999). Six ATPases are involved in unfolding and linearizing the deubiquitinated protein and also opening the gate for protein entry into the narrow pore of the 20S core complex (Glickman & Ciechanover, 2002).

The proteolytic 20S core is barrel-shaped and contains enzymes that play a crucial role in degrading the protein into smaller oligopeptides (Voges et al., 1999). The α-type subunits form the two seven-member outermost rings that surround the central pore where the targeted proteins enter and the fragmented peptides exit (Lecker et al., 2006) (Figure 2). Within the barrel-shaped core are two seven-member innermost rings composed of β-type subunits, where three of the subunits positioned on the interior side of the core contain proteolytic activity (Figure 2). Polypeptides that enter the 20S core are cleaved into smaller peptides that exit the proteasome (Lecker et al., 2006). The specific size of degraded peptides ranges from approximately 4 to 25 residues (Wenzel, Eckerskorn, Lottspeich, & Baumeister, 1994). The digested peptides are either further degraded into their respective amino acids by endopeptidases and aminopeptidases

located in the cytoplasm, or used in antigen presentation (Lecker et al., 2006).

The 26S proteasome can be transported throughout the cytosol or nucleus using specific localization signals, depending on where its function is needed (Kawahara & Yokosawa, 1992; Amsterdam, Pitzer, & Baumeister, 1993). For example, the 26S proteasome may be targeted to a cellular region that contains abnormal or damaged proteins or oncogenes (Coux, Tanaka, & Goldberg, 1996; Lee & Goldberg, 1998; Huibregtse, Maki, & Howley, 1998).

1.2) E3 Ubiquitin Ligases

Substrate specificity provided by the E3 ubiquitin ligases is essential for the ubiquitination pathway to function properly. The importance of the ubiquitin ligase is reflected in the fact that the Arabidopsis genome contains more than 1400 distinct E3 enzymes, comprising a considerable portion of the predicted proteome (Smalle & Vierstra, 2004; Kraft et al., 2005). In addition to the large number and complex nature of E3 ligases that provide substrate specificity, the many potential combinations of ubiquitin conjugating enzymes and ubiquitin ligases allows for a variety in how ubiquitination occurs on a particular substrate (Stone et al., 2005).

E3 ubiquitin ligases are characterized according to the presence of E2-binding domains. There are three distinct groups of E3 ligases defined by the presence of a Homologous to E6-AP carboxyl terminus (HECT), U-box, or Really Interesting New Gene (RING) domain (Smalle & Vierstra, 2004; Stone et al., 2005) (Figure 3). HECT E3s are functionally different from the RING and U-box E3s because they form an E3-ubiquitin intermediate prior to transfer of ubiquitin onto the substrate (Verdecia et al.,

Figure 2. Structure of the 26S proteasome. The 26S proteasome consists of two 19S regulatory caps at each end of a 20S core complex. The 20S core contains two seven-member innermost rings composed of β-type subunits, and two outermost rings composed of α-type subunits. (Image taken from Google Images, retrieved on May 31st, 2015).

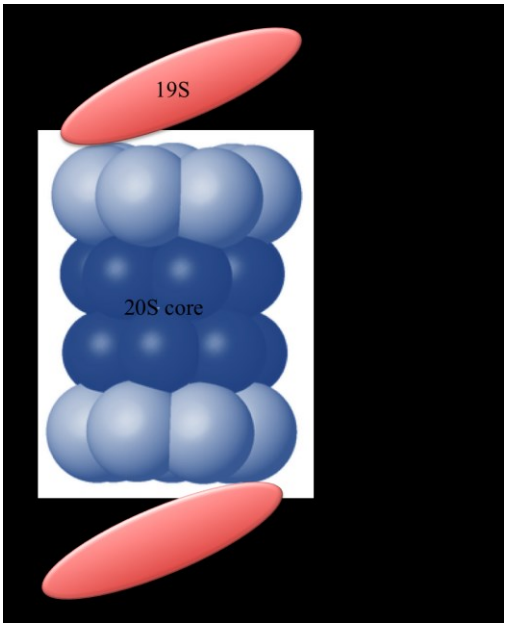
19S
20S core

2003). RING and U-box E3 ligases are structurally similar and facilitate transfer of ubiquitin to the selected substrate by assembling E2 and the substrate protein in close proximity to facilitate ubiquitin transfer (Verdecia et al., 2003).

RING-type E3 Ligases

RING domains are characterized by the presence of a 70 amino acid sequence that consists of an octet of cysteine and histidine residues that coordinates two zinc ions to form a cross brace structure (Pickart, 2001; Freemont, 1993; Zheng et al., 2000). Ubiquitin transfer from the E2 directly onto the substrate is dependent on the proper folding of this cross brace structure (Freemont, 1993). The RING domain is used to bind the E2-ubiquitin intermediate, while another motif or domain is used to interact with the substrate. RING-type E3 ligases can be either monomeric or multimeric, where they contain E2- and substrate binding functions within the same protein, or on separate proteins, respectively (Figure 3) (Deshaies & Joazeiro, 2009; Smalle & Vierstra, 2004). The Arabidopsis genome encodes for more than 470 proteins that contain a RING domain and can function as monomeric RING-type E3 ligase (Stone et al., 2005; Kraft et al., 2005). Based on the presence of the different types of substrate binding domains, the Arabidopsis monomeric RING-type E3 ligase family can be classified into thirty different subgroups (Stone et al., 2005). Domains used by RING-type E3 ligases to facilitate substrate binding via protein-protein interactions include ankyrin (ANK), domain homologous to E6 associated protein carboxy-terminus and RCC1 domain protein (HERC repeats), Breast cancer 1, early onset (BRCA1) C terminus (BRCT), and beta-transducin repeats (WD40) (Stone et al., 2005).

Figure 3. Schematic representation of E3 ubiquitin ligases HECT, U-box, and RING. These E3 ligases are characterized based on the presence of E2-binding domains. RING-type E3 ligases can be monomeric or multimeric proteins. Monomeric E3 ligases are composed of E2- and substrate binding functions within the same protein, whereas these functions reside on separate proteins in multimeric ligases. A well-known example of a multimeric RING E3 includes the superfamily of cullin RING ligases (CRL). Within this superfamily, Skp1, Cullins, F-box protein (SCF) cullin RING ligase 1 (CRL1) family contains a cullin protein (Cullin RING ligase 1 (Cul1)), a RING box protein 1 (Rbx1) that binds to E2, an adaptor protein S-phase kinase-associated protein 1 (Skp1) that binds to F-box proteins, which recognize specific substrates (Image taken from Metzger et al., 2014).

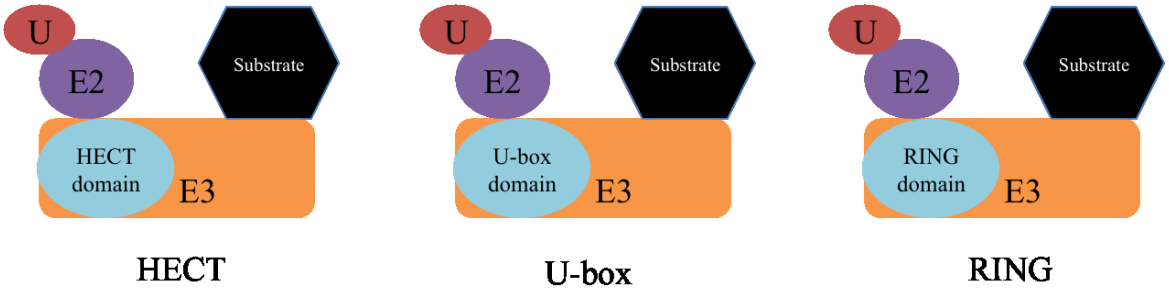

HECT **U-box** **RING**

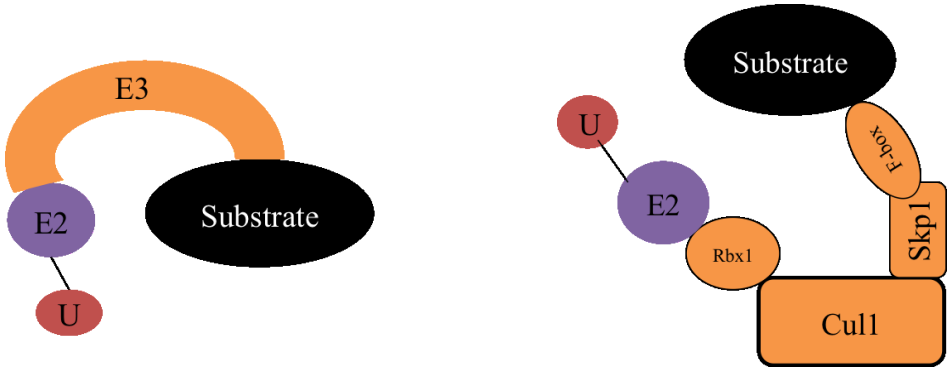

Monomeric RING-type E3 ligases

Multimeric RING-type E3 ligases

RING-ankyrin E3 Ligase Family

There are six members of the RING domain-containing ankyrin (RING-ankyrin) E3 ligase group including XA21-binding protein 3 (XB3) ortholog in *Arabidopsis thaliana* (XBAT)31, XBAT32, XBAT33, XBAT34, XBAT35, and XBAT36, all of which are structurally similar to the *Oryza sativa* (rice) XB3 (Stone et al., 2006; Nodzon et al., 2004) (Figure 4). XB3 is an E3 ubiquitin ligase that interacts specifically with the XA21 serine and threonine kinase substrate (Wang et al., 2006). XB3 consists of a series of ankyrin repeats and a RING-finger motif, both of which function to interact with the XA21 kinase domain (Wang et al., 2006). XB3 is involved in pathogen defense in *Oryza sativa* (rice) (Ronald et al., 1992; Song et al., 1995; Wang et al., 2006). Each member of the RING-ankyrin group contains a RING domain and a series of ankyrin repeats (Stone et al., 2006; Kraft et al., 2005) (Figure 4). Each ankyrin (ANK) repeat consists of 30-34 amino acids that play a role in mediating protein-protein interactions (Li et al., 2006; Sedgwick & Smerdon, 1999). Although the biological functions of all members of the RING-ankyrin E3 ligase group are still not yet determined, biological roles can be assigned to XBAT32 and XBAT35 (Nodzon et al., 2004; Lyzenga et al., 2012; Prasad et al., 2010; Prasad & Stone, 2010; Yuan et al., 2013). XBAT32 is involved in the positive regulation of lateral root development and cellular responses to abiotic stresses using an ethylene-mediated mechanism. Lateral root development is mediated by the down-regulation of ethylene biosynthesis, achieved in part by XBAT32-mediated degradation of ethylene biosynthetic enzymes (Nodzon et al., 2004; Lyzenga et al., 2012; Prasad et al., 2010; Prasad & Stone, 2010; Yuan et al., 2013). XBAT35 is involved in the negative regulation of apical hook curvature via ethylene signaling (Carvalho et al., 2012; Yuan et

Figure 4. Arabidopsis RING-type ankyrin E3 ligase family. This family consists of XBAT31-35. Arabidopsis XBAT proteins are structurally similar to rice XB3. Each protein contains a RING domain and a series of amino terminal ankyrin (ANK) repeats (Image taken from Yuan et al., 2013).

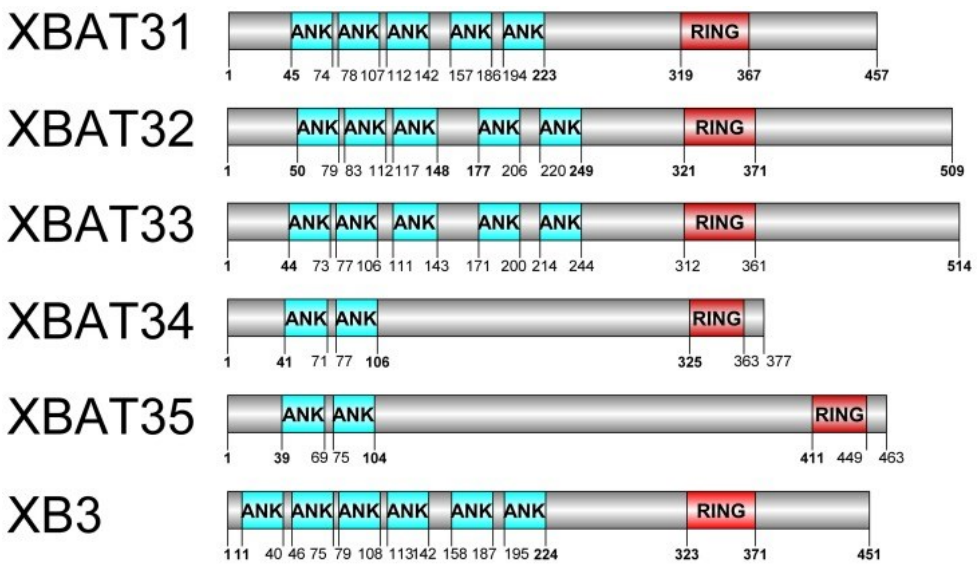
XBAT31
ANK ANK ANK ANK ANK RING
1 45 74 78 107 112 142 157 186 194 223 319 367 457
XBAT32
ANK ANK ANK ANK ANK RING
1 50 79 83 112 117 148 177 206 220 249 321 371 509
XBAT33
ANK ANK ANK ANK ANK RING
1 44 73 77 106 111 143 171 200 214 244 312 361 514
XBAT34
ANK ANK RING
1 41 71 77 106 325 363 377
XBAT35
ANK ANK RING
1 39 69 75 104 411 449 463
XB3
ANK ANK ANK ANK ANK ANK RING
1 11 40 46 75 79 108 113 142 158 187 195 224 323 371 451

al., 2013).

1.3) XB3 ortholog in *Arabidopsis thaliana* (XBAT) 35

XBAT35 is a member of the RING-ankyrin E3 ligase subgroup (Yuan et al., 2013; Stone et al., 2005; Nodzon et al., 2004). A unique characteristic of *XBAT35* is an exon skipping alternative splicing event of the transcript that generates two proteins, where one larger variant localizes to the nucleus (XBAT35.1) and the other smaller variant lacks the nuclear localization signal (NLS) (XBAT35.2) (Carvalho et al., 2012) (Figure 5). The XBAT35.2 isoform was also recently found to localize to the Golgi in addition to the cytosol (Liu et al., unpublished results). Evidence to support whether or not XBAT35.2 localizes inside or outside the Golgi is lacking. The *XBAT35* gene contains 10 exons and 9 introns, and alternate splicing results in the skipping of exon 8 to generate an mRNA transcript that lacks the portion of the transcript encoding for the NLS. Both isoforms of XBAT35 are functional E3 ligases and play an important role in ethylene signaling as a negative regulator of apical hook curvature (Carvalho et al., 2012). Both XBAT35.1 and XBAT35.2 are structurally similar with the exception of 24 amino acids including the NLS, and have no differences in expression patterns as constitutive expression across all plant tissues occurs (Carvalho et al., 2012). The significance of the alternative splicing event is for differential localization of the two isoforms, where both proteins are involved in regulating apical hook via ethylene-mediated signaling in their respective compartments (Carvalho et al., 2012). Evidence for both isoforms performing similar functions has been established when expression of either XBAT35.1 or XBAT35.2 was able to rescue apical hook exaggeration in *XBAT35*

Figure 5. Schematic representation of the Arabidopsis RING E3 ligases, XBAT35.1 and XBAT35.2. *XBAT35* produces two protein isoforms following alternative splicing, XBAT35.1 and XBAT35.2. Exon 8 is retained in the XBAT35.1 mRNA transcript, which encodes for a nuclear localization signal (NLS). Alternative splicing that results in exon 8 skipping generates the other protein isoform, XBAT35.2. XBAT35.2 is targeted to the Golgi apparatus. Both isoforms contain two ankyrin repeats (ANK) followed by an E2 binding RING domain (Image taken from Carvalho et al., 2012).

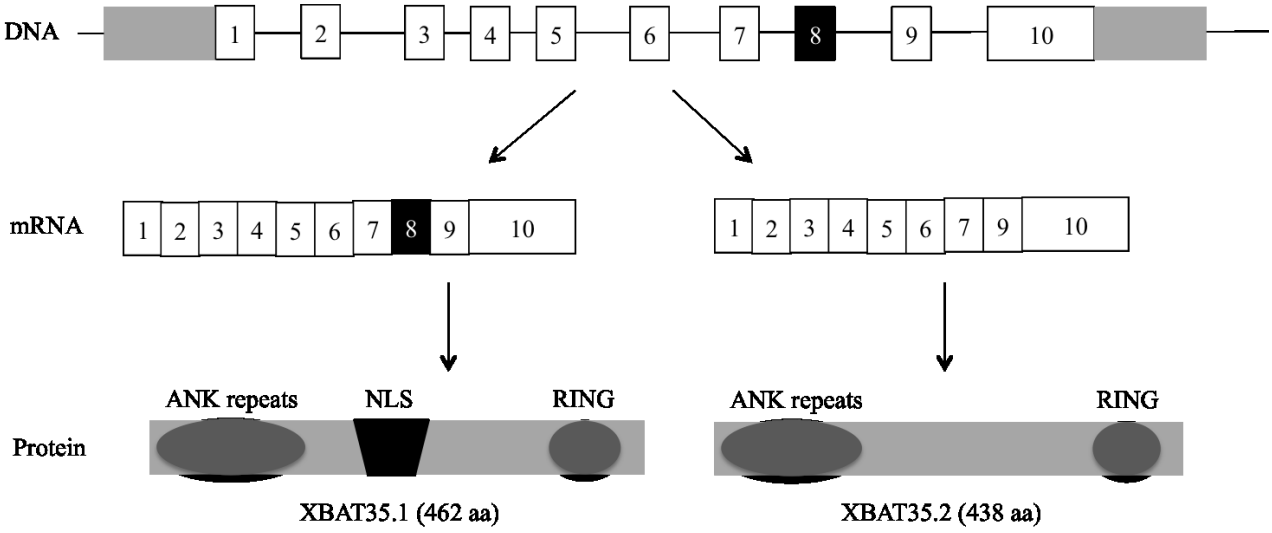
DNA
1
2
3
4
5
6
7
8
9
10
mRNA
1
2
3
4
5
6
7
8
9
10
1
2
3
4
5
6
7
9
10
Protein
ANK repeats
NLS
RING
ANK repeats
RING
XBAT35.1 (462 aa)
XBAT35.2 (438 aa)

Figure 6. XBAT35 Interaction map. This predicted network of association between XBAT35 and ACD11 in *Arabidopsis thaliana* was determined using the GeneMania software (http://www.genemania.org). Searches were carried out on May 29th, 2015. Black nodes are indicative of query genes. Pink lines indicate physical interactions that are based on experimental data; orange lines indicate interactions based on predictions; purple lines indicate co-expression; green lines indicate shared protein domain organization. XBAT31 was also included in the predicted network of associated due to its domain similarity to XBAT35. Accession numbers: *XBAT35,* At3g23280; *ACD11*, At2g34690; *GLTP2*, At1g21360; *GLTP3*, At3g21260; *GLTP1,* At2g33470; *GLTP*, At4g39670; *PRA1.F2*, At1g55190; *PRA1.F3*, At3g13720; *BPA1*, At5g16840; *PRA1.F4*, At3g13710; *VAP27*, At3g60600; *ANK1*, At5g02620; *ANK,* At5g60070, *ANK*, At1g05640; *XBAT32*, *At5g57740; EMB139,* At5g40160; *F18O22,* At5g14230; *TIP1,* At5g20350; *AT4G19150/T18B16,* At4g19150; *XBAT31,* At2g28840; *EMB16,* At5g66055; *ACBP1,* At5g53470.

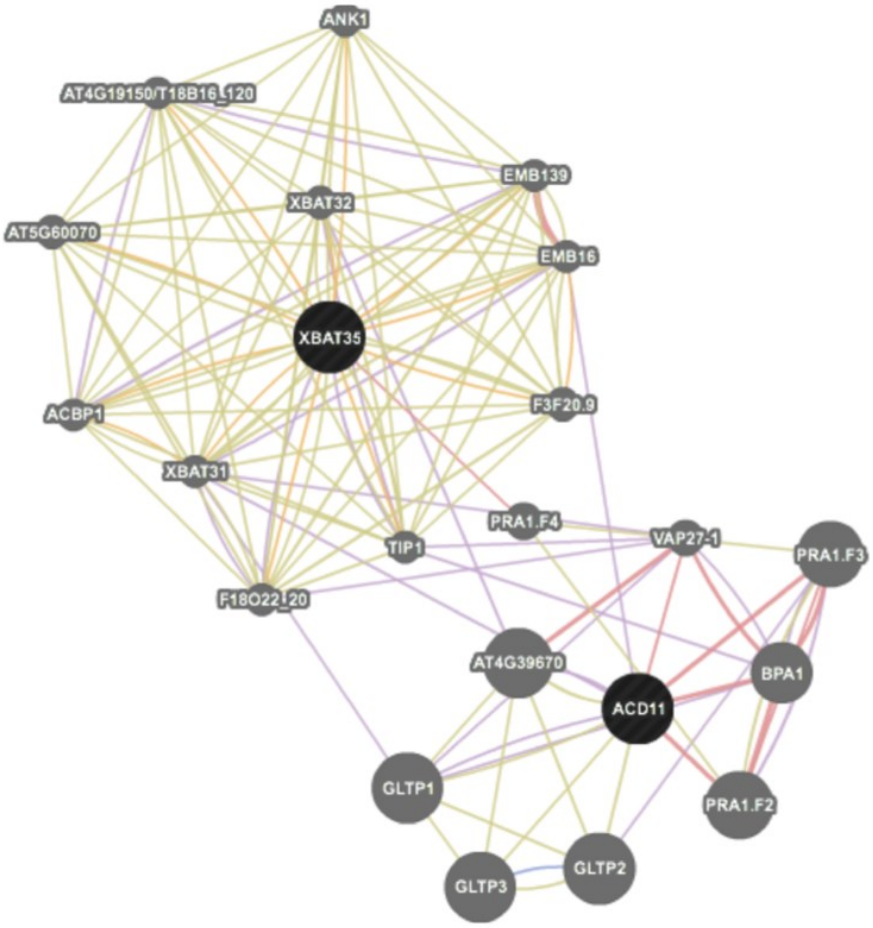
ANK1
AT4G19150/T18B16_120
EMB139
XBAT32
AT5G60070
EMB16
XBAT35
F3F20.9
ACBP1
XBAT31
PRA1.F4
VAP27-1
PRA1.F3
TIP1
F18O22_20
AT4G39670
BPA1
ACD11
GLTP1
PRA1.F2
GLTP2
GLTP3

Figure 7. BiFC showing the interaction between XBAT35.2 and ACD11 in tobacco leaf epidermal cells. After transient co-expression of XBAT35.2 ^{AA}-YN and ACD11-YC in tobacco leaf epidermal cells, YFP fluorescence was observed, indicating an interaction between the two fusion proteins. Left panels show fluorescence image from a single optical section. Middle panels show transmitted light image. Right panels show transmitted light image merged with fluorescence image. Bars = 50 μm. (Liu et al., unpublished).

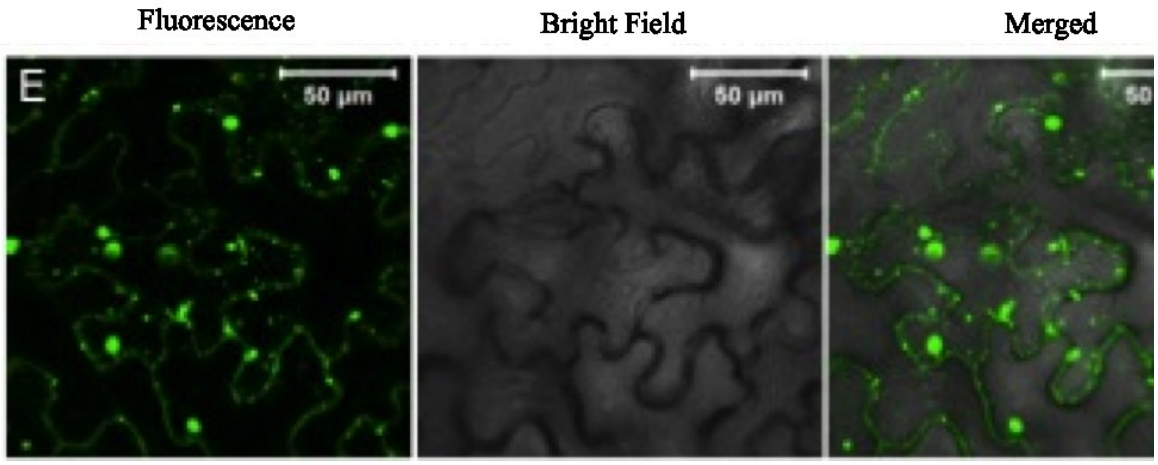
Fluorescence
Bright Field
Merged
E
50 µm
50 µm

mutants in an ethylene-dependent manner (Carvalho et al., 2012).

Searches of public protein-protein interaction databases, such as Gene Mania (http://www.genemania.org) and BioGrid (http://thebiogrid.org), identified a number of potential interacting partners for XBAT35 (Figure 6) based on shared protein domain organization (Liu et al., unpublished results). Previous results from a yeast-two hybrid screen suggest an interaction between XBAT35.2 and the Golgi-localized *Arabidopsis thaliana* Prenylated Rab acceptor 1 (AtPRA1-F) proteins involved in vesicle trafficking, which are also shown to interact with the pathogen-related Accelerated Cell Death 11 (ACD11) in a yeast-two-hybrid analysis (Petersen et al., 2009; Liu et al., unpublished results). Another hypothesized potential interactor for XBAT35.2 includes ACD11, which is of particular interest (Figure 6). To provide evidence for this potential interaction, bimolecular fluorescence complementation assays (BiFC) were used to demonstrate that the XBAT35 isoform, XBAT35.2, interacts with ACD11 in plant cells (Liu et al., unpublished) (Figure 7). For BiFC, ACD11 was expressed as a fusion protein with the carboxyl portion (YC) of the yellow fluorescence protein (YFP) (ACD11-YC), while XBAT35.2 was expressed as a fusion protein with the amino portion (YN) of YFP (XBAT35.2-YN). Also, an inactive version of XBAT35.2 (XBAT35.2^{AA}-YC) was also used in the BiFC assay, where two point mutations, cysteine 426 and histidine 428 to alanine, disrupted the E3 ligase activity. The presence of a fluorescence signal following transient co-expression of each fusion protein in tobacco leaf epidermal cells indicates that the YFP was reconstituted due to interactions between ACD11 and XBAT35.2 (Figure 7). XBAT35.2 was found to interact with ACD11 mainly at punctate structures within the cell, which were determined to be Golgi (Figure 7) (Liu et al., unpublished

results).

1.4) Accelerated Cell Death 11 (ACD11)

ACD11 encodes for a 22.7 kD sphingosine transfer protein that can accelerate the transfer of sphingosine and sphingomyelin across intermembranes (Simanshu et al., 2014; Brodersen et al., 2002; Petersen et al., 2008). ACD11 is also involved in programmed cell death (PCD), an active process that results in the controlled destruction of cells to inhibit the spread of pathogens (Moon et al., 2004; Simanshu et al., 2014; Pennell & Lamb, 1997). Sphingosines consist of an unsaturated hydrocarbon chain and are an important structural component of sphingolipids. Sphingolipids are found in eukaryotic membranes and are involved in the regulation of plant PCD (Simanshu et al., 2014). Previous research on *Fusarium* and *Alternaria* fungal pathogen species shows that toxins produced by the fungus kill plant cells by disturbing enzyme activity in sphingolipid biosynthesis pathways (Takahashi et al., 2009). In the sphingolipid biosynthesis pathway, metabolites including ceramide (Cer), ceramide-1-phosphate (C1P), long chain bases (LCB), and sphingosine and sphingosine-1-phosphate (S1P) are messenger signals involved in regulating PCD (Fyrst & Saba, 2010; Hannun & Obeid, 2008; Michaelson, 2010; Simanshu et al., 2014). Specifically, the relationship between Cer and C1P metabolites is the most important dynamic balance in PCD regulation (Berkey et al., 2012; Chen, 2009; Pata et al., 2010; Reape & McCabe, 2008; Simanshu et al., 2014). The *acd11* null mutant in Arabidopsis has a defect in the gene that encodes for a sphingosine transfer protein, which results in elevated levels of total sphingolipids, but ceramide species, which are inducers of PCD, have the most significant accumulation (Simanshu et al., 2014). These

findings suggest that ACD11 mediates the synthesis of sphingolipid metabolites, specifically Cer (Simanshu et al., 2014).

Programmed Cell Death

Two different methods of achieving cell death in multicellular organisms include necrosis and programmed cell death (PCD). PCD is a genetically defined active process that involves specific signaling pathways and results in cellular control of degeneration, whereas necrosis lacks tightly regulated mechanisms and results in cellular death following traumatic damage to cells (Brodersen et al., 2002). In plants, PCD occurs at specific stages of development, during pathogen interaction that results in disease symptoms, and during the hypersensitive response that occurs as a result of avirulent stress effectors (Lam, 2004; Simanshu et al., 2014). Common cases where PCD is involved in developmental processes include cell senescence and sex determination (Pennell & Lamb, 1997; Brodersen et al., 2002). In both avirulent infections and disease development with virulent infections in plants, PCD is observed (Morel & Dangl, 1997; Brodersen et al., 2002). In both instances, resistance genes encode for plant proteins that play a role in activating cell death during the hypersensitive response following infection. When infection is perceived, this leads to a cellular response that results in the activation of resistance and pro-death pathways (Shirasu & Schultze-Lefert, 2000; Brodersen et al., 2002). Examples of hypersensitive cellular responses include accumulation of reactive oxygen species, salicylic acid, and nitric oxide (Simanshu et al., 2014). Local accumulation of these factors in the hypersensitive response contributes to defensive resistance in affected plant tissue in order to prevent the spread of infection that would

eventually kill the whole plant (Shirasu & Schultze-Lefert, 2000; Brodersen et al., 2002).

Previous genetic studies suggest that there are two groups of signaling components involved in the hypersensitive response during pathogen infection. During a hypersensitive response, the first group of mutants does not respond to avirulent pathogens (Brodersen et al., 2002). Of interest is the second group in Arabidopsis, *acd* lethal, recessive mutants, which constitutively activates defense responses in the absence of pathogens, and thus mimics a hypersensitive cellular response (Brodersen et al., 2001). Pathogen resistance and defense related genes are thus continuously expressed (Simanshu et al., 2014). Examples of defense related genes include the *Pathogenesis-related (PR)* genes, *PR1* and *PR2* (Brodersen et al., 2002). Arabidopsis *acd11* plants generate seeds that germinate and develop cotyledons, but at the two- to six-leaf stage chlorotic tissue forms and further development ceases (Brodersen et al., 2002). *ACD11* therefore inhibits cell death in the absence of pathogens by suppressing the constitutive expression of *acd11*. Plants that lack the functional *ACD11* gene are usually capable of reaching the seedling stage, but survival beyond this developmental stage is limited due to the fact that PCD and defense signaling pathways are activated even in the absence of pathogens (Brodersen et al., 2002). *acd11* serves as a valuable genetic model for the activation of immune responses and preventing the spread of pathogens during plant infections via localized cellular suicide (Simanshu et al., 2014).

XBAT35.2 and Programmed Cell Death

Preliminary analyses indicate that ACD11 interacts with XBAT35.2, which suggests that the E3 ligase may also play a role in pathogen defense and PCD (Liu et al.,

unpublished results). The transient overexpression of XBAT35.2 resulted in induction of cell death in tobacco leaf epidermal cells (Figure 8) (Liu et al., unpublished results). Overexpression of XBAT35.1 did not induce cell death in tobacco cells (Liu et al., unpublished results) (Figure 8). This provides evidence for a role for XBAT35.2 in PCD. In addition, the E3 ligase activity of XBAT35.2 is required for PCD induction because overexpression of a mutant version of XBAT35.2 (XBAT35.2^{AA}) with an inactive RING E3 ligase domain failed to induce cell death (Figure 8). The observed cell death or lack thereof are also not attributed to differences in protein expression because western blot analysis from protein extracts from infiltrated tissue shows that each protein is expressed at a similar level (Figure 8) (Liu et al., unpublished results). Importantly, transgenic Arabidopsis plants overexpressing XBAT35.2 showed enhanced resistance to pathogen (Liu et al., unpublished results). These results provide initial evidence for a role of XBAT35.2 RING E3 ligase in PCD and pathogen defense.

1.5) Role of E3 Ligases in Pathogen Defense

Examples of pathogen proteins being regulated by E3 ligases have been well characterized (Furlan et al., 2012; Duplan & Rivas, 2014; Dreher & Callis, 2007; Turner et al., 2002; Kim & Delaney, 2002; Durrant et al., 2000; van den Burg et al., 2008; Craig et al., 2009). A well-described example involves *Arabidopsis* flagellin-sensitive 2 (FLS2) ubiquitination by U-box-type E3 ligases, Plant U-Box12 (PUB12) and PUB13 (Göhre et al., 2008; Lu et al., 2011). FLS2 is a pattern-recognition receptor (PRR), which is a receptor that is able to recognize bacterial and viral pathogens and activate innate immune responses (Lu et al., 2011). FLS2 plays an important role in sensing flagellin,

which is a critical component found in bacterial flagella. Flagellin is also a virulence factor that is easily recognized by plant innate immune systems (Hayashi et al., 2001; Lu et al., 2011). At the molecular level, PUB12 and PUB13 E3 ligases are recruited by flagellin at a receptor complex that includes FLS2 and Brassinosteroid insensitive 1-associated kinase 1 (BAK1). BAK1 is responsible for phosphorylating the E3 ligases, PUB12 and PUB13, before they interact with and polyubiquitinate FLS2, signaling it for degradation (Lu et al., 2011). Flagellin treatments where mutations in the genes encoding for the E3 ligases are present result in elevated immune responses, as E3 ligase activity of *pub12* and *pub13* is inactive (Lu et al., 2011). Polyubiquitination and degradation of FLS2 can therefore not occur, which enables the activation and initiation of immune signaling. Similarly, when FLS2 is mutated, *Arabidopsis* becomes more susceptible to bacterial infections (Zipfel et al., 2004; Craig et al., 2009, Göhre et al., 2008). These findings provide strong evidence for the biological role of E3 ligases in pathogen defense.

1.6) Purpose of Study

The purpose of this research project is to determine the significance of the interaction between the RING-ankyrin E3 ligase, XBAT35.2 and ACD11. Although, similar to ACD11, evidence is provided to support a role for XBAT35.2 in pathogen resistance, it is not known if ACD11 is a *bona fide* substrate for the E3 ligase. The aim of this study is to 1) confirm the interaction between XBAT35.2 and ACD11, 2) determine if ACD11 is degraded by the UPS, and 3) demonstrate that XBAT35.2 E3 ligase is involved in targeting ACD11 for degradation by the 26S proteasome. This research will enhance our understanding of the biological role of XBAT35.2 during biotic

stress response. Characterizing the relationship between XBAT35.2 and ACD11 provides an opportunity to further expand our knowledge on the molecular basis of programmed cell death and pathogen resistance in plants. The research may be of significance to the agriculture sector where plants with enhanced pathogen resistance can be produced, which could potentially result in major economical benefits.

Figure 8. Tobacco leaves illustrating cell death following transient expression of yellow florescence protein (YFP) tagged XBAT35.2. Sites of Agrobacterium mediated infiltration are indicated by circles in A and B. Tobacco leaves were transiently transformed with plant transformation plasmids which allow for expression of YFP-XBAT35.1 (A), YFP-XBAT35.2 (A and B) or RING mutant YFP-XBAT35.2^{AA} (B). Immunoblot analysis was used to detect transgene expression using GFP antibodies (A and B; right panels) 72 hours after infiltration (Liu et al., unpublished results).

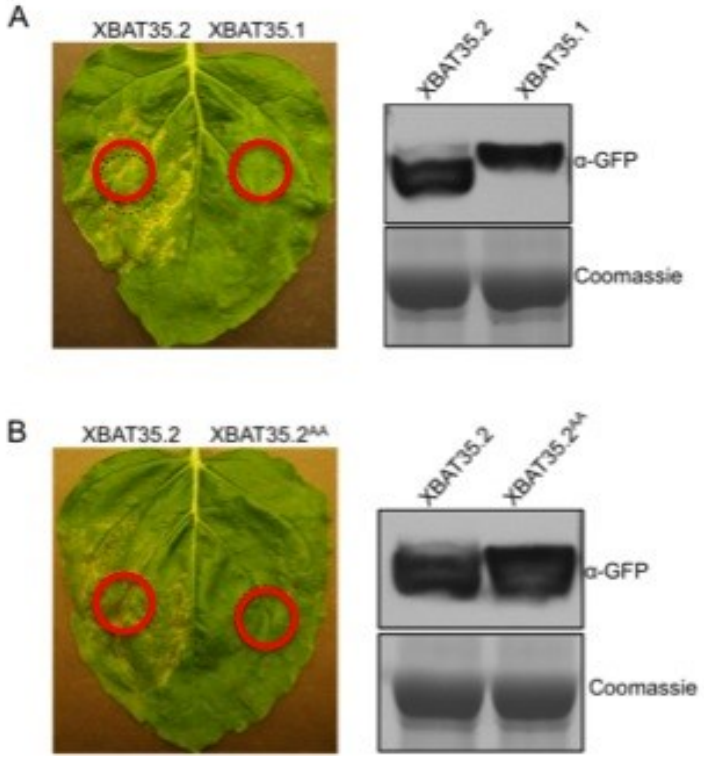
A
XBAT35.2
XBAT35.1
XBAT35.2
XBAT35.1
α-GFP
Coomassie
B
XBAT35.2
XBAT35.2AA
XBAT35.2
XBAT35.2AA
α-GFP
Coomassie

Chapter 2: Materials and Methods

2.1) Transient Protein Expression in *Nicotiana benthamiana*

Previously, full-length *ACD11* (At2g34690) cDNA were obtained from the Arabidopsis Biological Resource Center (ABRC) (Alonso et al., 2003). The full-length cDNA of *XBAT35.2* (At3g23280) was obtained by reverse transcription (RT)-PCR. All cDNAs were introduced into the Gateway ® entry vector pDONR201 (Invitrogen) as per manufacturer's instructions and nucleotide sequences were confirmed by DNA sequencing (McGill University and Génome Québec Innovation Centre) (Liu et al., unpublished). For XBAT35.2^{AA}, the site-directed mutagenesis (Finnzymes) was used to make two point mutations, cysteine 426 and histidine 428 to alanine, within the RING domain-encoding region of the cDNA. *XBAT35.2* and *XBAT35.2^{AA}* cDNAs in the entry vector pDONR201 were introduced into the pEarleyGate201 plant transformation vector (Earley et al., 2006) using Gateway cloning (Invitrogen) to produce in-frame fusions with the yellow fluorescence protein (YFP) tag (YFP-XBAT35.2 and YFP-XBAT35.2^{AA}) under the control of the cauliflower mosaic virus 35S promoter. Similarly, *ACD11* cDNA was cloned into the pEarleyGate101 vector to generate the YFP and hemagglutinin (HA) tag fusion (YFP-HA-ACD11).

I grew *Nicotiana benthamiana* (tobacco) plants in a 23°C growth chamber for six weeks prior to transient protein expression and co-expression. The photoperiod fluctuated between 16 hours of light and 8 hours of dark (Sparkes et al., 2006). I carried out transient expression of fusion proteins in tobacco plants as previously described (Sparkes et al., 2006). Briefly, I transformed *Agrobacterium tumefaciens* GV3101 with plant transformation vectors, pEarley Gate 101or pEarley Gate 201, containing the coding

region for *ACD11* or *XBAT35.2/XBAT35.2^{AA}*, respectively. I harvested Agrobacterium cultures and then resuspended in an infiltration solution containing 5 mg/ml D-glucose, 50 mM MES, 2 mM Na_3PO_4, and 0.1 mM acetosyringone. I adjusted the resulting bacterial suspension with infiltration solution to an optical density (OD) of OD_{600}≈0.8. For co-infiltration, I mixed Agrobacterium suspensions transformed with the plasmids containing the coding regions for *XBAT35.2/XBAT35.2^{AA}* or *ACD11* in a 60:40 ratio, respectively. I used a needleless syringe to introduce the Agrobacterium suspensions into the underside of leaves of six-week-old tobacco plants. I collected infiltrated tobacco leaves after 48 hours for protein extraction and stored the tissue at -80°C. Immunoblot analysis (described below) using GFP or HA antibodies was used to confirm expression of the fusion proteins in infiltrated tobacco tissue. GFP antibodies are able to detect the YFP tag fused to the proteins of interest.

2.2) Protein Extraction and Immunoblot Analysis

I used protein extraction buffer (including HEPES pH 7.5, 5 mM EDTA, 5 mM EGTA, 10 mM Na_3VO_4, 10 mM NaF, 50 mM β-glycerophosphate, 10 mM dithiothreitol, 1 mM phenylmethylsulfonyl fluoride, 5% glycerol and protease inhibitor cocktail (Sigma-Aldrich)) to extract the total protein content from infiltrated tobacco tissue. I centrifuged the samples for 5 minutes at 18,000 g and the resulting supernatant was transferred to a new Eppendorf tube. I added 6x Sodium dodecyl sulfate (SDS) loading buffer (300 mM Tris-HCl pH 6.8, 30% glycerol, 12% SDS, 0.6% Bromophenol Blue) to each sample, boiled for 5 minutes and centrifuged at 18, 000 g for 5 minutes, prior to loading on 7.5% SDS polyacrylamide gel (SDS-PAGE). Following loading, each gel was

electrophoresed at 125V for 85 minutes. I then transferred proteins from the polyacrylamide gel to polyvinylidene fluoride (PVDF) membrane using a semi-dry electro-transfer unit. Following protein transfer, I blocked the PVDF membrane with 5% milk solution and TBST (50 mM Tris-HCl, pH7.5, 150 mM NaCl and 0.05% Tween 20) for 1 hour at room temperature. I then incubated PVDF with primary antibody for 2 hours, followed by three 10-minute washes with TBST. I added secondary antibody for 1 hour, followed by an additional three 10-minute washes with TBST. The specific types of primary and secondary antibodies I used in the incubations depended on the tags fused to the proteins of interest (Table 1). I then visualized the proteins of interest using an Enhanced Chemiluminescence (ECL) Western Blotting Substrate kit as per manufacturer's instructions (Thermo Scientific).

2.3) Immunoprecipitation Assay (IP)

I used total protein extracted from un-infiltrated (control tissue) and infiltrated/co-infiltrated tobacco leaves expressing YFP-HA-ACD11 and/or YFP-XBAT35.2/XBAT35.2^{AA} for immunoprecipitation assays. I added 20 µl of HA beads, prepared according to manufacturer's instructions (Sigma-Aldrich), to protein extracts and incubated the samples for 2-6 hours at 4°C. After incubation, I collected the HA-beads using centrifugation followed by two washes with TBS (50 mM Tris-HCl, pH7.5, 150 mM NaCl). After the final wash, I collected HA-beads using centrifugation and I added 30 µl of 1X SDS to each sample. I boiled the samples for 5 minutes and loaded them onto SDS-PAGE gels. I used immunoblot analysis using GFP and HA antibodies to detect the isolated fusion proteins.

2.4) Cell Free Degradation Assay

Cell free degradation assays were performed as previously described (Wang et al., 2009). Briefly, I extracted total protein from infiltrated tobacco leaves expressing YFP-HA-ACD11, YFP-XBAT35.2 or YFP-XBAT35.2^{AA}. For the cell free degradation assay, I mixed protein extracts containing ACD11 and YFP-XBAT35.2 or YFP-XBAT35.2^{AA} and added 100 mM ATP to each reaction at time zero followed by incubation at 30°C. I removed equal volumes of each reaction at the indicated time points and added 6x SDS loading buffer to stop the reaction. For assays with proteasome inhibitor treatment, I divided protein extracts equally into 2 separate tubes and added 30 μM MG132 (Sigma-Aldrich) to one tube, while I added equal volume of protein extraction buffer to the other tube (control). I added MG132 to the assay 30 minutes before the addition of ATP. After sample collection at each time point, I determined protein levels of YFP-HA-ACD11 and/or YFP-XBAT35.2 / XBAT35.2 ^{AA} using immunoblot analysis with the appropriate primary and secondary antibodies (see Table 1). I used ImageJ (http://imagej.nih.gov/ij/) to estimate the percentage of protein remaining at each time point (Abramoff, Magalhaes & Ram, 2004).

Table 1: List of primary and secondary antibodies (Sigma-Aldrich) used to detect YFP and HA fusion proteins in immunoblotting analysis.

Protein tags	Primary antibody	Secondary antibody	Dilution
YFP	Rabbit anti-GFP (Sigma-Aldrich)	Horseradish peroxidase-conjugated goat anti-rabbit (Sigma-Aldrich)	1:5000
HA	Mouse anti-HA (Sigma-Aldrich)	Anti-mouse (Sigma-Aldrich)	1:5000

Chapter 3: Results

3.1) ACD11 interacts with XBAT35.2

Immunoprecipitation assays were performed to provide further support for the proposed interaction between ACD11 and XBAT35.2. Figure 9 shows the results of the immunoprecipitation assays, where YFP-XBAT35.2^{AA} was isolated with YFP-HA-ACD11. In order to prevent ubiquitination and thus subsequent degradation of the interacting proteins by the 26S proteasome, the function of the RING domain of XBAT35.2 was rendered inactive by introducing two point mutations (cysteine 426 and histidine 428) to alanine (XBAT35.2^{AA}) (Stone et al., 2006). Despite the E3 ligase activity being rendered inactive, protein binding to the substrate can still occur. HA-beads were used to immunoprecipitate YFP-HA-ACD11 from protein extracts that were prepared from tobacco leaf tissue transiently expressing YFP-HA-ACD11 alone (lane 1), or co-expressing YFP-HA-ACD11 and YFP-XBAT35.2^{AA} (lane 2). Also, protein extracts from tobacco leaves expressing ACD11 or XBAT35.2^{AA} were mixed and used in immunoprecipitation assays (lane 3). The results show that ACD11 is capable of pulling down XBAT35.2, which confirms interaction between the two proteins (Figure 9).

3.2) ACD11 is stable when expressed alone in tobacco cells

ACD11 interaction with the RING-type E3 ligase, XBAT35.2, is an indication that the ubiquitin-proteasome system may potentially play a role in regulating the abundance of ACD11. Cell free degradation assays were conducted in order to assess the stability of YFP-HA-ACD11 in the presence and absence of proteasome inhibitor, MG132 (Figure 10 and 11). If ACD11 is degraded by the UPS then YFP-HA-ACD11

abundance is expected to decrease over time in the absence of MG2132, while remaining stable in the presence of the proteasome inhibitor. The abundance of YFP-HA-ACD11 remained fairly consistent in the absence (-MG132) and presence (+MG132) of proteasome inhibitor over time (Figure 10). In repeated assays, the abundance of YFP-HA-ACD11 again remained consistent over time in the absence of MG132 (Figure 11). For each trial, the ImageJ software was used to quantify the abundance of YFP-HA-ACD11 remaining at each indicated time point relative to the zero time point. As shown, the percentage of ACD11 remaining at each time point did not change significantly (Figure 10 and 11), suggesting that the protein is not targeted for degradation by the UPS. Although only two results are shown as representatives, the stability of ACD11 when expressed alone in tobacco cells was repeatable across four experiments.

3.3) ACD11 is degraded in the presence of a functional XBAT35.2

To assess whether the abundance of ACD11 remains stable in the presence of a functional XBAT35.2 E3 ligase, tobacco leaf tissue co-expressing YFP-HA-ACD11 and YFP-XBAT35.2 were used in cell free degradation assays. In two separate trials, ACD11 abundance was found to decrease over time in the presence of YFP-XBAT35.2 (Figure 12 and 13). Quantification of the level of YFP-HA-ACD11 remaining at each indicated time point demonstrates a significant decrease in ACD11 protein levels (Figure 12 and 13). To determine if the observed ACD11 turnover is dependent on the XBAT35.2 E3 ligase activity, cell free degradation assays were carried out using an inactive E3 ligase, XBAT35.2^{AA}. In the presence of the E3 ligase with an inactive RING domain, the previously observed degradation of ACD11 did not occur (Figure 12 and 13). These

results demonstrate that the E3 ligase activity of XBAT53.2 is required for ACD11 degradation.

3.4) Degradation of ACD11 in the presence of XBAT35.2 is due to the 26S proteasome

The protein abundance of ACD11 decreases over time in the presence of a functional XBAT35.2. In order to determine if the observed degradation of ACD11 is due to the 26S proteasome, a cell free degradation assay was used to assess the stability of ACD11 in the presence of functional XBAT35.2 with or without proteasome inhibition. As expected, in the presence of the proteasome inhibitor, MG132, the rate of ACD11 degradation is significantly reduced (Figure 14 and 15). In the absence of MG132, proteasome activity regulates normally, and ACD11 is degraded at a faster rate. These results demonstrate that the degradation of ACD11 in the presence of a functional RING E3 ligase, XBAT35.2, is proteasome dependent.

3.5) The RING E3 ligase, XBAT35.2, is unstable

The results shown in Figure 12 and Figure 13 indicate that the functional RING-type E3 ligase was also unstable and is turned over by the 26S proteasome. Degradation of XBAT35.2 did not occur when the RING domain of the E3 ligase was mutated and non-functional (XBAT35.2 ^{AA}), or the proteasome inhibitor, MG132, was included in the assay (Figure 12, 13 and 14). These assays presented in Figure 12, 13 and 14 were carried out in the presence of ACD11, therefore, the stability of XBAT35.2 was next assessed in cell free degradation assays without ACD11. Also, to determine whether XBAT35.2 is

capable of self-ubiquitination, a cell free degradation assay was used to compare the turnover of YFP-XBAT35.2 and YFP-XBAT35.2 ^{AA} (Figure 16). The levels of YFP-XBAT35.2 gradually decreased over time, while the protein levels of YFP- XBAT35.2 ^{AA} remained fairly stable over the same time period (Figure 16). These results indicate that XBAT35.2 is unstable and capable of self-ubiquitination as the non-functional E3 ligase is not degraded.

Taken together, these results indicate that the abundance of ACD11 is regulated by the ubiquitin proteasome system, and XBAT35.2 is involved in promoting the degradation of ACD11 in a 26S proteasome-dependent manner.

Figure 9. Immunoprecipitation assay (IP) showing interaction between ACD11 and XBAT35.2. Protein extracts from tobacco tissue transiently expressing YFP-HA-ACD11 (lane 1), co-expressing YFP-HA-ACD11 and YFP-XBAT35.2^{AA} (lane 2), or extracts from tissue expressing YFP-HA-ACD11 or YFP-XBAT35.2 ^{AA} were mixed (lane 3) and used in IP assays. Western blot analysis using GFP antibody was used to detect both YFP-HA-ACD11 and YFP-XBAT35.2^{AA}.

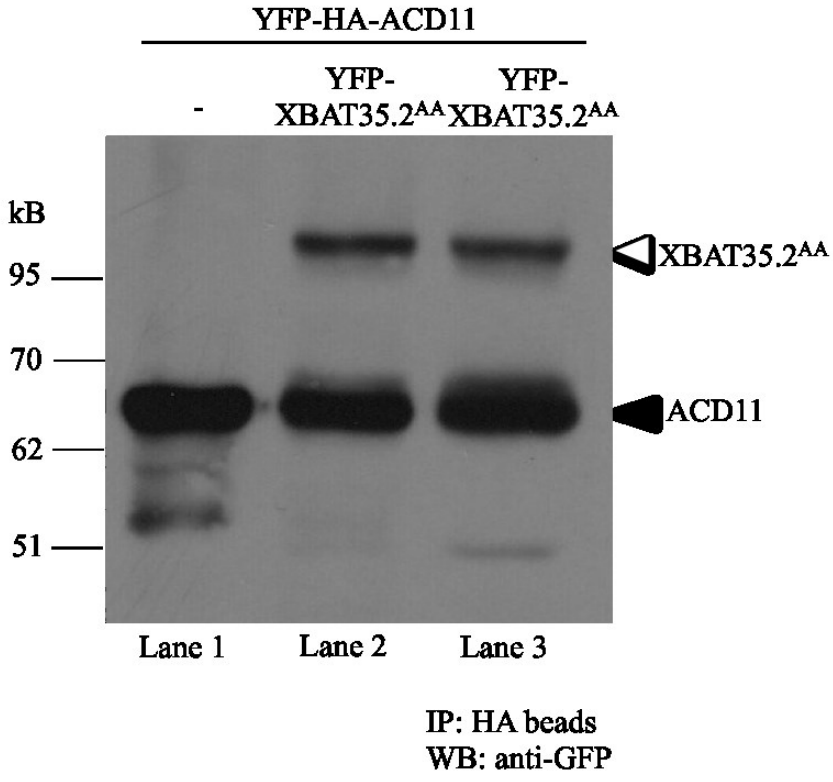
YFP-HA-ACD11
-
YFP-XBAT35.2AA
YFP-XBAT35.2AA
kB
95
70
62
51
XBAT35.2AA
ACD11
Lane 1
Lane 2
Lane 3
IP: HA beads
WB: anti-GFP

Figure 10: ACD11 is stable in a cell free degradation assay. Cell free degradation assays were carried out using protein extracts prepared from transiently transformed tobacco leaves expressing ACD11-HA-YFP treated with (+) or without (-) 30 μM MG132. The levels of ACD11 remaining at the indicated time points were determined by western blot (WB) analysis using GFP antibodies. Percent (%) remaining) was calculated using ImageJ software. (min - minutes).

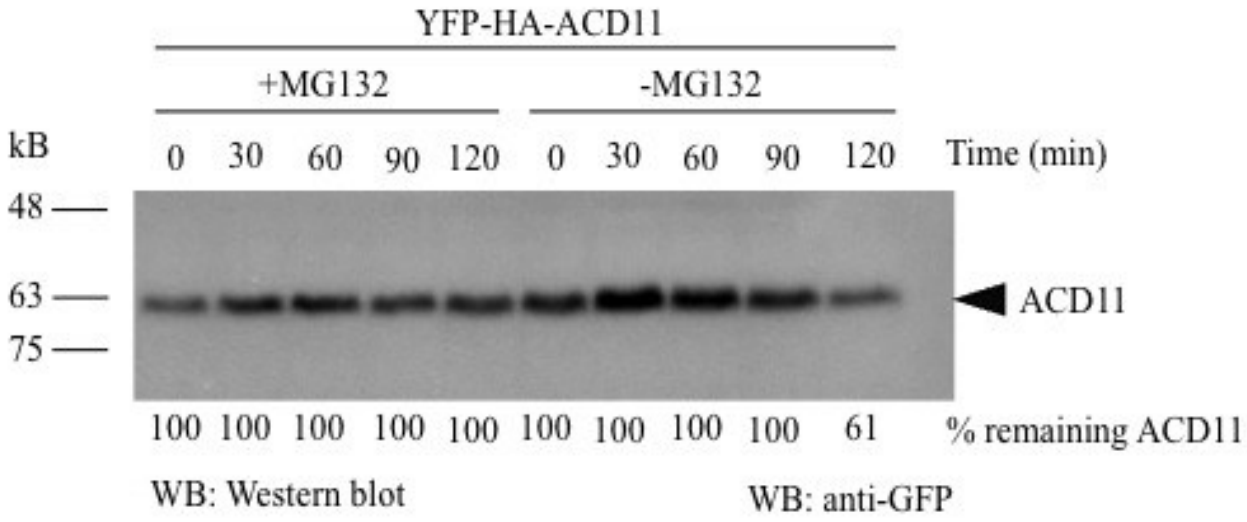
YFP-HA-ACD11
+MG132
-MG132
kB
0 30 60 90 120 0 30 60 90 120
Time (min)
48
63
75
ACD11
100 100 100 100 100 100 100 100 100 61
% remaining ACD11
WB: Western blot
WB: anti-GFP

Figure 11: Repeat of cell free degradation assay showing ACD11 stability. Cell free degradation assays were carried out using protein extracts prepared from transiently transformed tobacco leaves expressing YFP-HA-ACD11. The levels of YFP-HA-ACD11 remaining at the indicated time points were determined by western blot (WB) analysis using GFP antibodies. Percent (%) remaining was calculated using ImageJ software. Ponceau S staining shows protein loading. (min - minutes).

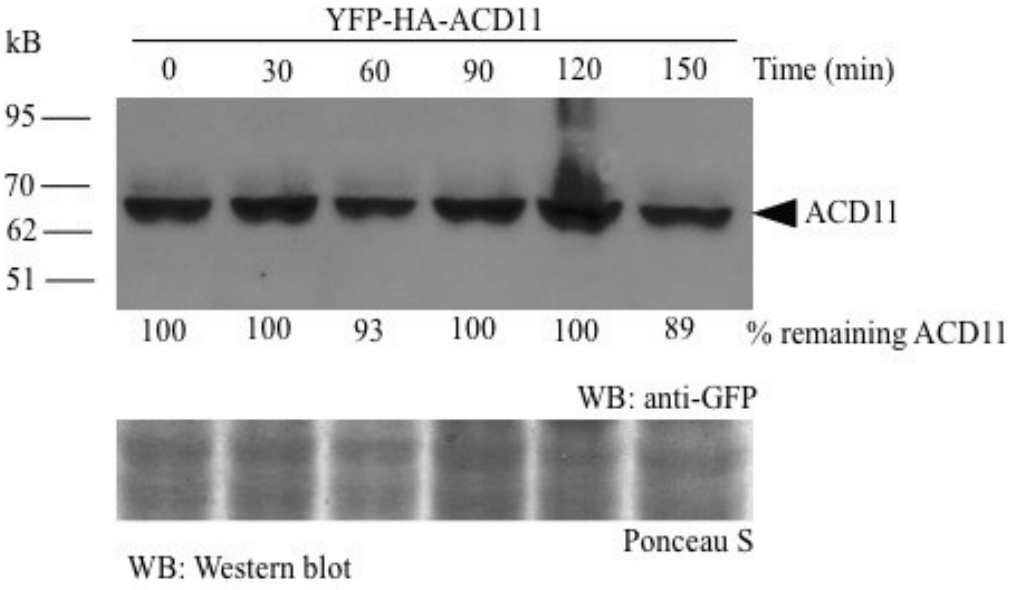
YFP-HA-ACD11
kB
0
30
60
90
120
150
Time (min)
95
70
62
51
ACD11
100
100
93
100
100
89
% remaining ACD11
WB: anti-GFP
Ponceau S
WB: Western blot

Figure 12: Degradation of ACD11 in the presence of XBAT35.2. Protein extracts prepared from transiently transformed tobacco leaves containing YFP-HA-ACD11 mixed with extracts containing YFP-XBAT35.2 or YFP-XBAT35.2 ^{AA} and used in cell free degradation assays. Western blot (WB) analysis using GFP antibodies was used to detect YFP-HA-ACD11, YFP-XBAT35.2, or YFP-XBAT35.2^{AA} simultaneously. Percent (%) remaining was calculated using ImageJ software. Ponceau S staining shows protein loading. (min - minutes).

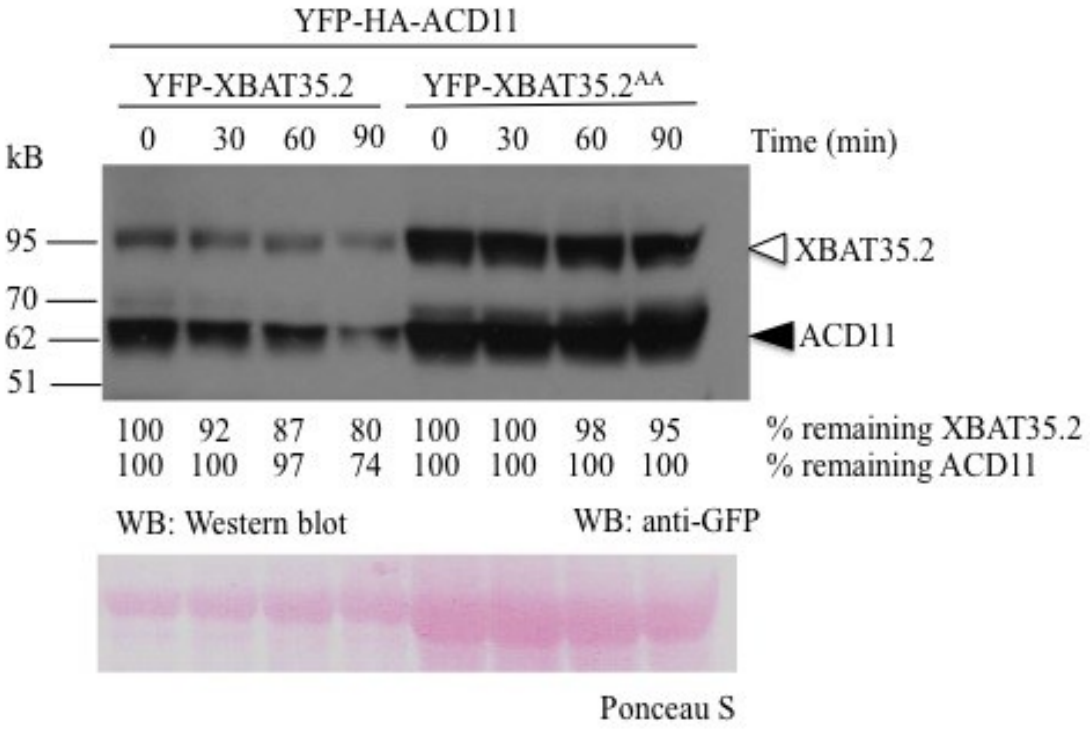
YFP-HA-ACD11
YFP-XBAT35.2
YFP-XBAT35.2AA
0 30 60 90 0 30 60 90
Time (min)
kB
95
70
62
51
XBAT35.2
ACD11
100 92 87 80 100 100 98 95
% remaining XBAT35.2
100 100 97 74 100 100 100 100
% remaining ACD11
WB: Western blot
WB: anti-GFP
Ponceau S

Figure 13: Repeat of cell free degradation assays showing turnover of ACD11 in the presence of XBAT35.2. Protein extracts prepared from transiently transformed tobacco leaves containing YFP-HA-ACD11 mixed with extracts containing YFP-XBAT35.2 or YFP-XBAT35.2 ^{AA} and used in cell free degradation assays. Western blot (WB) analysis using GFP antibodies was used to detect YFP-HA-ACD11, YFP-XBAT35.2 and YFP-XBAT35.2^{AA} simultaneously. Percent (%) remaining was calculated using ImageJ software. Ponceau S staining shows protein loading. (min - minutes).

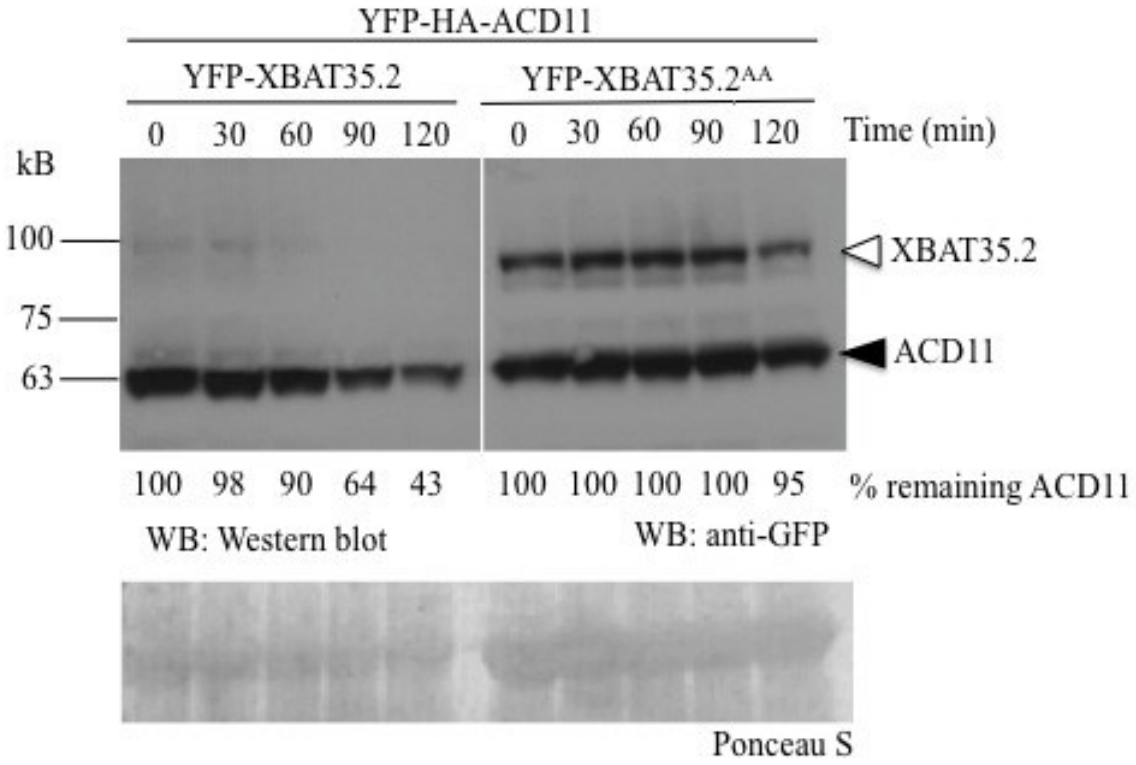
YFP-HA-ACD11
YFP-XBAT35.2
YFP-XBAT35.2AA
0 30 60 90 120
0 30 60 90 120
Time (min)
kB
100
75
63
XBAT35.2
ACD11
100 98 90 64 43
100 100 100 100 95
% remaining ACD11
WB: Western blot
WB: anti-GFP
Ponceau S

Figure 14: XBAT35.2 mediated degradation of ACD11 requires the 26S proteasome. Protein extracts prepared from transiently transformed tobacco leaves containing YFP-HA-ACD11 mixed with extracts containing YFP-XBAT35.2, treated with (+) or without (-) MG132, were used in cell free degradation assays. Western blot (WB) analysis using GFP antibodies was used to detect YFP-HA-ACD11 and YFP-XBAT35.2 simultaneously. Percent (%) remaining was calculated using ImageJ software. Ponceau S staining shows protein loading. (min - minutes).

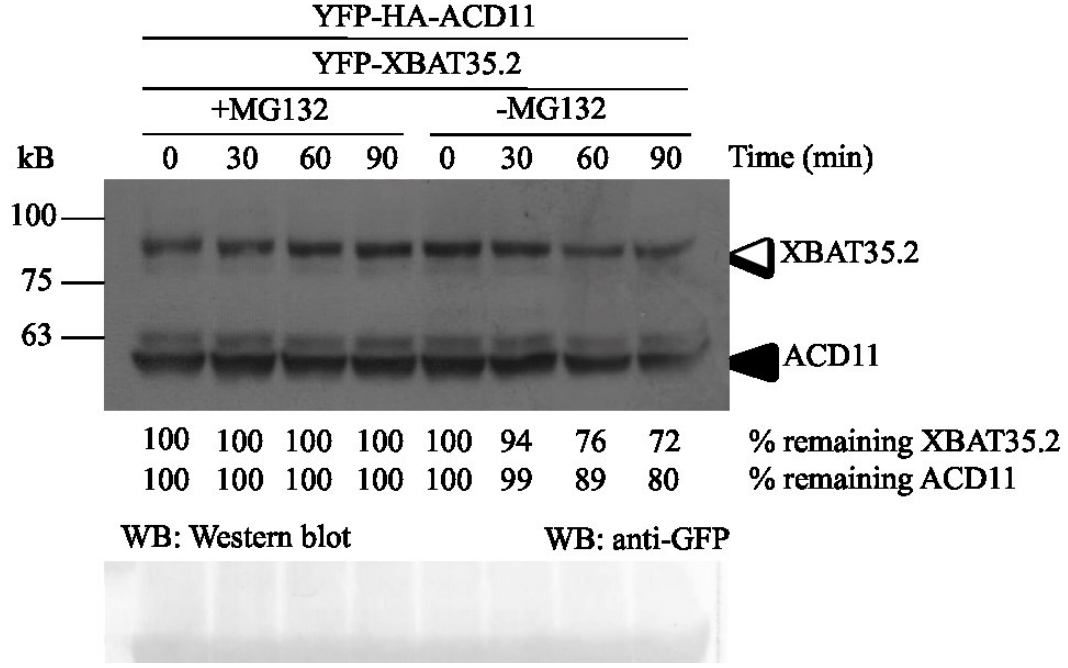
YFP-HA-ACD11
YFP-XBAT35.2
+MG132
-MG132
kB
0 30 60 90 0 30 60 90
Time (min)
100
75
63
XBAT35.2
ACD11
100 100 100 100 100 94 76 72 % remaining XBAT35.2
100 100 100 100 100 99 89 80 % remaining ACD11
WB: Western blot
WB: anti-GFP

Figure 15: Repeat of cell free degradation assay showing that XBAT35.2 mediated degradation of ACD11 requires the 26S proteasome. Protein extracts prepared from transiently transformed tobacco leaves containing YFP-HA-ACD11 mixed with extracts containing YFP-XBAT35.2 treated with (+) or without (-) MG132, were used in cell free degradation assays. Western blot (WB) analysis using GFP antibodies was used to detect YFP-HA-ACD11. Percent (%) remaining was calculated using ImageJ software. (min - minutes).

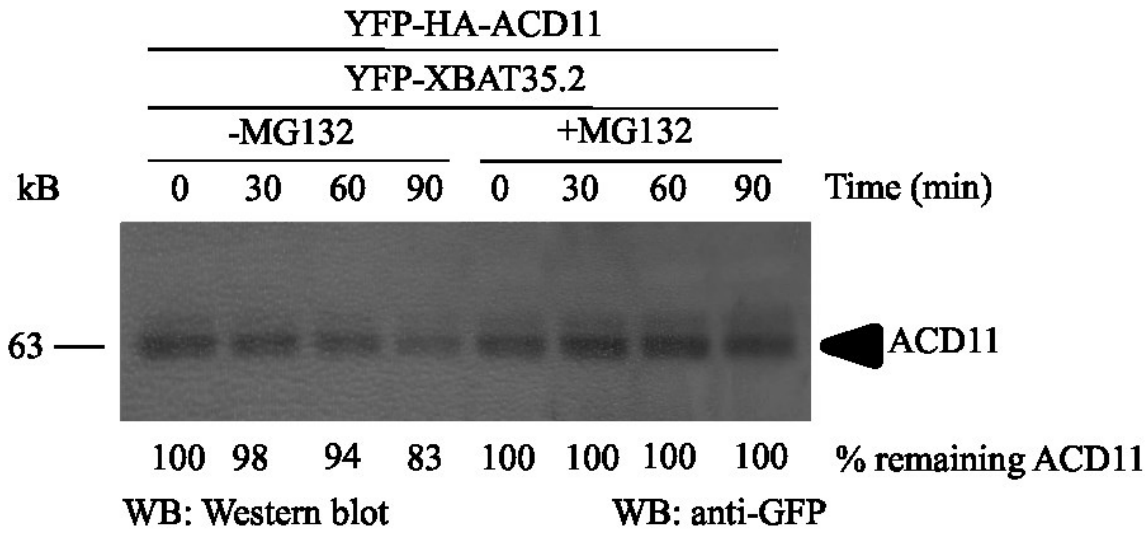
YFP-HA-ACD11
YFP-XBAT35.2
-MG132
+MG132
kB
0 30 60 90 0 30 60 90
Time (min)
63
ACD11
100 98 94 83 100 100 100 100
% remaining ACD11
WB: Western blot
WB: anti-GFP

Figure 16: Turnover of XBAT35.2 in cell free degradation assays. Protein extracts prepared from transiently transformed tobacco leaves containing YFP-XBAT35.2 or YFP-XBAT35.2^{AA} were used in cell free degradation assays. Western blot (WB) analysis using GFP antibodies was used to detect YFP-XBAT35.2 and YFP-XBAT35.2^{AA}. Percent (%) remaining was calculated using ImageJ software. Ponceau S staining shows protein loading. (min - minutes).

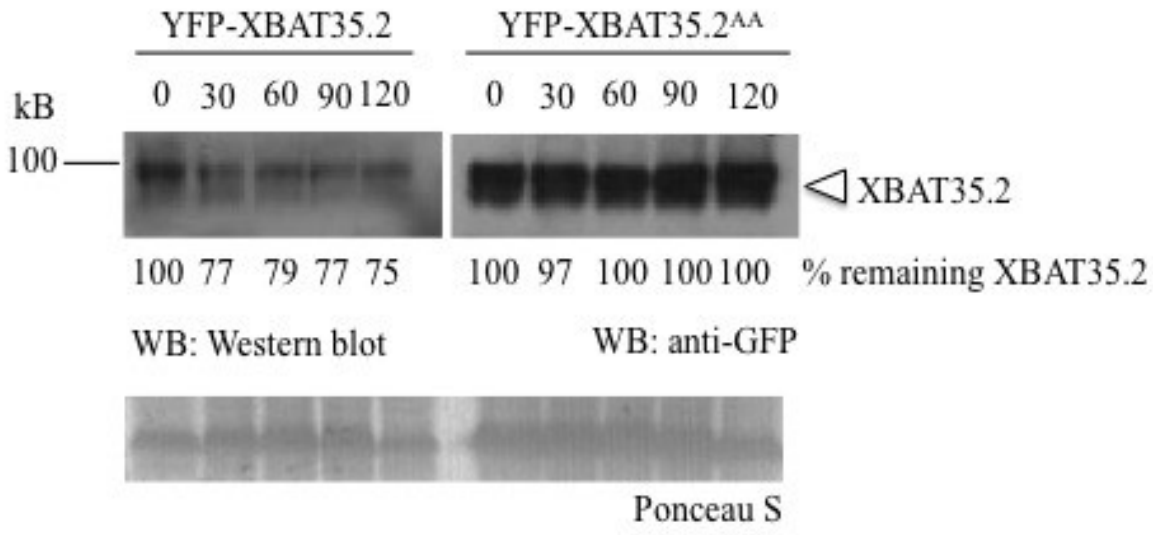
YFP-XBAT35.2
YFP-XBAT35.2AA
0 30 60 90 120
0 30 60 90 120
kB
100
XBAT35.2
100 77 79 77 75
100 97 100 100 100
% remaining XBAT35.2
WB: Western blot
WB: anti-GFP
Ponceau S

Chapter 4: Discussion

4.1) Evidence for interaction between XBAT35.2 and ACD11

Results obtained from previous high throughput yeast-two-hybrid screens suggest that the RING-type E3 ligase XBAT35 interacts with ACD11 (Brodersen et al., 2002; Petersen et al., 2009; Braun et al., 2011). In accordance, a BiFC assay shows that XBAT35.2 and ACD11 interact at punctate structures in tobacco leaf epidermal cells (Figure 7). Although the BiFC assays provide strong evidence for *in planta* interaction between XBAT35.2 and ACD11, the use of the constitutive 35S promoter to drive expression may produce false results due to the high abundance of the fusion proteins within the cell. Therefore, an alternative method was used to confirm interaction between XBAT35.2 and ACD11. Further evidence for the interaction between XBAT35.2 and ACD11 was confirmed by IP assays (Figure 9), which show that YFP-HA-ACD11 was able to interact with and pull down YFP-XBAT35.2^{AA}. HA-beads were used to isolate YFP-HA-ACD11 from protein extracts prepared from tobacco leaf tissue transiently expressing YFP-HA-ACD11 or YFP-XBAT35.2^{AA}. In all cases, YFP-XBAT35.2^{AA} was detected along with YFP-HA-ACD11 following IP with HA beads. These results provide strong evidence in support of the interaction between the RING-type E3 ligase, XBAT35.2, and ACD11.

4.2) XBAT35.2 promotes proteasomal-dependent degradation of ACD11

I also showed that XBAT35.2 promotes the degradation of ACD11 in a 26S proteasome-dependent manner (Figure 14 and 15). Cell free degradation assays using protein extracts from tobacco tissue transiently expressing YFP-HA-ACD11 mixed with

extracts containing transiently expressed YFP-HA-XBAT35.2 or XBAT35.2^{AA} resulted in a decreased abundance of ACD11 in the presence of the functional E3 ligase (Figure 12 and 13). Proteasomal-dependent degradation of ACD11 was subsequently determined as degradation of ACD11 in the presence of functional XBAT35.2 occurred at a significantly slower rate with proteasome inhibition using MG132 (Figure 14 and 15). These results demonstrate that ACD11 is a substrate for XBAT35.2 E3 ligase activity.

In plants where the gene function of *ACD11* is mutated or suppressed, constitutive activation of programmed cell death and defense signaling pathways occurs regardless of whether or not pathogen is present (Brodersen et al., 2002). Due to continuous activation of defense signaling pathways, plant survival beyond the seedling stage is limited (Brodersen et al., 2002). Phenotypic indicators of PCD activation and cellular defense mechanisms include chlorotic patches, as seen at the two-leaf stage in the recessive lesion mimic mutant, *acd11* (Brodersen et al., 2002). In addition, regulation of gene expression in *acd11* results in Pathogenesis-related (PR) genes, *PR1* and *PR2*, being expressed constitutively. Up-regulation of pathogenesis-related proteins encoded by *PR1* and *PR2* are indicative of activated defense signaling pathways (Brodersen et al., 2002). Similar to *acd11* lesion mimic mutants, overexpressing the functional E3 ligase, XBAT35.2, in tobacco leaf tissue results in cell death phenotypes (Figure 8) and increased pathogen resistance in Arabidopsis plants (Liu et al., unpublished results). Together, these results suggest that XBAT35.2 plays a role in plant innate immunity and programmed cell death by regulating the abundance of ACD11.

There is also evidence to suggest that XBAT35.2-mediated turnover of ACD11 occurs when a pathogen is present. ACD11 is quite stable when expressed in tobacco

cells, suggesting that ACD11 is not targeted to the UPS. However, in the presence of increased abundance of XBAT35.2, ACD11 is turned over by the 26S proteasome. Also, in the absence of *Pst* DC3000 pathogen, *xbat35-1* and transgenic plants over expressing XBAT35.2 developed similarly to wild type plants (Liu et al., unpublished results). Cellular defense responses were not activated as chlorosis was not detected in any of the mutant or transgenic plants, which suggests that programmed cell death and pathogen defense pathways were not activated (Liu et al., unpublished results). These findings contrast with *acd11* null mutants, which constitutively express defense-related genes and show signs of cell death early on in development, even in the absence of pathogens. We speculate that the presence of pathogens results in the accumulation of XBAT35.2 and subsequent degradation of ACD11 through the UPS, which triggers cellular defense responses.

4.3) Self-regulation of the RING-type E3 ligase XBAT35.2

I also showed that the RING-type E3 ligase is able to regulate its own abundance by self-ubiquitination and proteasome-dependent degradation (Figure 16). Catalysis of their own ubiquitination is a common characteristic of RING-type E3 ligases and can serve as a self-regulatory mechanism (de Bie & Ciechanover, 2011; Lorick et al., 1999; Huibregtse et al., 1995). The cell free degradation assay using protein extracts from tobacco tissue transiently expressing YFP-XBAT35.2 and YFP-XBAT35.2^{AA} showed a decrease in protein abundance of the functional XBAT35.2 but not the non-functional XBAT35.2^{AA} (Figure 16). This suggests that self-ubiquitination and degradation depends on its own RING E3 ligase activity. Although the significance of this self-regulation is

not fully understood, XBAT35.2 self-ubiquitination would be expected to maintain low levels of the E3 ligase until a stimulus such as pathogen attack is perceived by the cell.

4.4) A model linking XBAT35.2, ACD11, and response to pathogens

Based on this study, in addition to previous research done, a possible explanation for the biological function of the RING-type E3 ligase, XBAT35.2, can be represented in a model (Figure 17). When no pathogen is present, self-ubiquitination maintains low levels of XBAT35.2. ACD11 degradation by the 26S proteasome does not occur, allowing ACD11 to accumulate and suppress the activation of cellular defense responses. When a pathogen is perceived, self-ubiquitination of XBAT35.2 discontinues and the RING-type E3 ligase accumulates. Stabilized XBAT35.2 then interacts with ACD11 and mediates ubiquitination of the substrate, targeting it to the 26S proteasome for degradation. Degradation of ACD11 allows for activation of cellular defense responses, resulting in pathogen defense (Figure 17).

This study was conducted in an attempt to fill in knowledge gaps regarding the interacting proteins of E3 ligases, as the biological functions of many E3 ligases have been determined through biochemical and transgenic studies but information on their interacting proteins is lacking. This research further supports the biological interaction between the RING-type E3 ligase, XBAT35.2, and ACD11, and identifies ACD11 as a ubiquitin substrate. The ubiquitinating activity of XBAT35.2 towards ACD11 in the presence of pathogens plays an important role in plant defense response pathways, as degradation of ACD11 promotes defense responses and results in localized cell death that

prevents further spread of pathogens. This study further supports the hypothesis that regulating defense responses is a major function of E3 ligases and the UPS.

Figure 17: A model explaining the interaction between XBAT35.2 and ACD11 in the presence and absence of pathogens. In the absence of pathogen, ACD11 ubiquitination is not mediated by XBAT35.2 because E3 ligase self-ubiquitination prevents the accumulation of the RING-type E3 ligase. ACD11 degradation by the 26S proteasome does not occur, which results in suppression of pathogen defense responses and the programmed cell death pathway. In the presence of a pathogen, self-ubiquitination of XBAT35.2 discontinues, which stabilizes the RING-type E3 ligase and enables binding to the substrate, ACD11. The ubiquitinating activity of XBAT35.2 towards ACD11 targets it to the 26S proteasome for degradation, which activates cellular defense responses and results in pathogen defense and enhanced resistance.

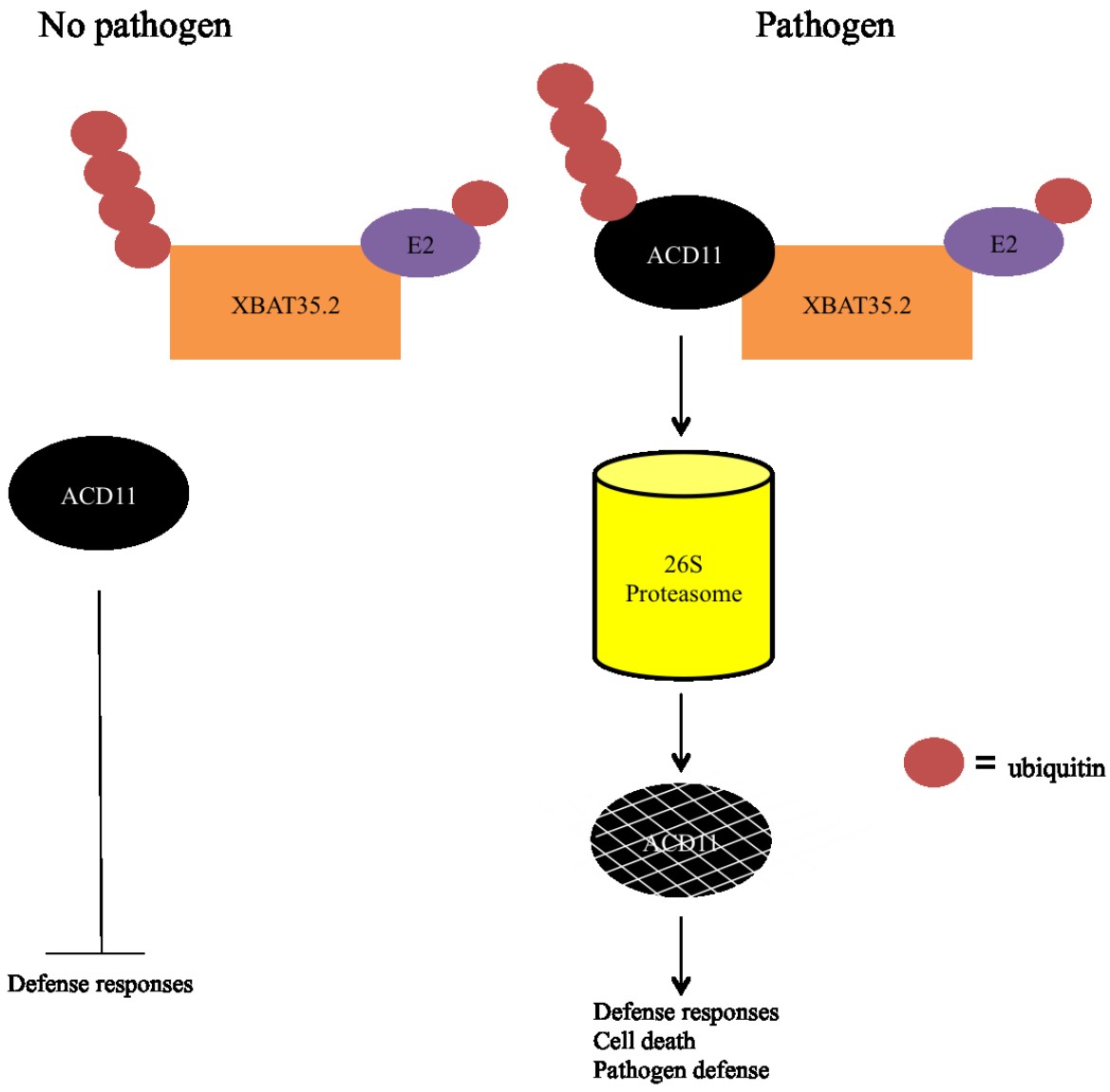
No pathogen
Pathogen
E2
XBAT35.2
ACD11
E2
XBAT35.2
ACD11
26S
Proteasome
= ubiquitin
ACD11
Defense responses
Defense responses
Cell death
Pathogen defense

References

Abramoff, M. D., Magalhaes, P. J., Ram, S. J. (2004). Image processing with ImageJ. *Biophotonics International,* 11(7), 36-42.

Alonso, J. M., Stepanova, A. N., Leisse, T. J., Kim, C. J., Chen, H., & Shinn, P., et al. (2003). Genome-wide insertional mutagenesis of *Arabidopsis thaliana. Science,* 301, 653-657.

Amsterdam, A., Pitzer, F., & Baumeister, W. (1993). Changes in the intracellular localization of proteasomes in immortalized ovarian granulosa cells during mitosis associated with a role in cell cycle control. *Proc Natl Acad Sci USA,* 90, 99-103.

de Bie, P., & Ciechanover, A. (2011). Ubiquitination of E3 ligases: self-regulation of the ubiquitin system via proteolytic and non-proteolytic mechanisms. *Cell Death Differ.,* 18(9), 1393-1402.

Berkey, R., Bendigeri, D., & Xiao, S. (2012). Sphingolipids and plant defense/disease: the "death" connection and beyond. *Frontiers Plant Sci.,* 3, 68.

Bonifacino JS, Dell'Angelica EC, Springer TA. (2001). Immunoprecipitation. *Curr Protoc Mol Biol.,*10.

Braun, P., Carvunis, A. R., Charloteaux, B., Dreze, M., Ecker, J. R., et al. (2011). Evidence for network evolution in an Arabidopsis interactome map. *Science,* 333, 601-607.

Brodersen P, Peterson M, Pike HM, Olszak B, Skov S, Odum N, et al. (2002). Knockout of *Arabidopsis ACCELERATED-CELL-DEATH11* encoding a sphingosine transfer protein causes activation of programmed cell death and defense. *Genes & Dev,* 16, 490-502.

Callis, J., Carpenter, T., Sun, C. W., & Vierstra, R. D. (1995). Structure and evolution of genes encoding polyubiquitin and ubiquitin-like proteins in Arabidopsis thaliana ecotype Columbia. *Genetics,* 139, 921-939.

Carvalho SD, Saraiva R, Maia TM, Abreu IA, Duque P. (2012). XBAT35, a novel Arabidopsis RING E3 ligase exhibiting dual targeting of its splice isoforms, is involved in ethylene-mediated regulation of apical hook curvature. *Mol Plant;* 5(6):1295-309.

Chen, Z. J., & Maniatis, T. (1998). Role of the ubiquitin-proteasome pathway in NF-kB activation. *Ubiquitin and the biology of the cell,* eds Peters J-M, Harris JR, Finley D. Plenum Press, New York, NY, pp 303-322.

Chen, M. C., Saucedo-Garcia, M., Plasencia, J., & Gavilanes-Ruiz, M. (2009). Plant sphingolipids: structure, synthesis, function. In: Wada H, editor. Lipids in Photosynthesis. New York: Springer; 2009. pp. 77-115.

Choi, S. W., Tamaki, T., Ebine, K., Uemura, T., Ueda, T., & Nakano, A. (2013). RABA members act in distinct steps of subcellular trafficking of the Flagellin Sensing2 receptor. *Plant Cell,* 25, 1174-1187.

Coux, O., Tanaka, K., & Goldberg, A. L. (1996). Structure and functions of the 20S and 26S proteasomes. *Annu Rev Biochem.,* 65, 801-847.

Craig, A., Ewan, R., Mesmar, J., Gudipati, V., & Sadanandom, A. (2009). E3 ubiquitin ligases and plant innate immunity. *J. Exp. Bot.,* 60(4), 1123-1132.

Deng, L., Wang, C., Spencer, E., Yang, L. Y., Braun, A., You, J. X., Slaughter, C., Pickart, C., & Chen, Z. J. (2000). Activation of the IkappaB kinase complex by TRAF6 requires a dimeric ubiquitin-conjugating enzyme complex and a unique polyubiquitin chain. *Cell,* 103, 351-361.

Deshaies J, and Joazeiro C. (2009). RING domain Ubiquitin Ligases. *Annu. Rev. Biochem*, 78: 399-434.

Dreher, K., Callis, J. (2007). Ubiquitin, hormones and biotic stress in plants. *Annals of Botany,* 99, 787-822.

Duplan, V., & Rivas, S. (2014). E3 ubiquitin-ligases and their target proteins during the regulation of plant innate immunity. *Front. Plant Sci.,* 5, 42.

Durrant, W. E., Rowland, O., Piedras, P., Hammond-Kosack, K. E., & Jones, J. D. (2000). cDNA-AFLP reveals a striking overlap in race-specific resistance and wound response gene expression profiles. *The Plant Cell,* 12, 963-977.

Earley, K. W., Haag, J. R., Pontes, O., Opper, K., Juehne, T., Song, K., Pikaard, C. S. (2006). Gateway-compatible vectors for plant functional genomics and proteomics. *Plant J.,* 45, 616-629.

Freemont PS. (1993). The RING finger. A novel protein sequence motif related to the zinc finger. *Ann. N. Y. Acad. Sci*., 684: 174-192.

Furlan, G., Klinkenberg, J., & Trujillo, M. (2012). Regulation of plant immune receptors by ubiquitination. *Front Plant Sci.,* 3, 238.

Fyrst, H., & Saba, J. D. (2010). An update on sphingosine-1-phosphate and other sphingolipid mediators. *Nat Chem Biol.,* 6, 489-497.

Genschik P, Criqui MC, Parmentier Y, Derevier A, and Fleck J. (1998). Cell Cycle-Dependent Proteolysis in Plants: Identification of the Destruction Box Pathway and Metaphase Arrest Produced by the Proteasome Inhibitor MG132. *The Plant Cycle;* 10:2063-2075.

Glickman MH, and Ciechanover A. (2002). The Ubiquitin 26S Proteasome Proteolytic Pathway. *Annual Review of Plant Biology;* 55(1):555-90.

Glickman, M. H., & Ciechanover, A. (2002). The ubiquitin-proteasome proteolytic pathway: destruction for the sake of construction. *Physiol Rev*, 82, 373-428.

Göhre, V., Spallek, T., Häweker, H., Mersmann, S., Mentzel, T., et al. (2008). Plant pattern-recognition receptor FLS2 is directed for degradation by the bacterial ubiquitin ligase AvrPtoB. *Curr Biol.,* 18, 1824-1832.

Haglund, K., Sigismund, S., Polo, S., Szymkiewicz, I., Di Fiore, P. P.,… et al. (2003). Multiple monoubiquitination of RTKs is sufficient for their endocytosis and degradation. *Nat. Cell Biol.,* 5, 461-466.

Haglund, K., Fiore, D., Dikic, I. (2003). Distinct monoubiquitin signals in receptor endocytosis. *Trends Biochem. Sci,* 28, 598-603.

Hannun, Y. A., & Obeid, L. M. (2008). Principles of bioactive lipid signaling: Lessons from sphingolipids. *Nat Rev Mol Cell Biol.,* 9, 139-150.

Hayashi, F., Smith, K. D., Ozinsky, A., Hawn, T. R., Yi, E. C., Goodlett, D. R., …& Aderem, A. (2001). The innate immune response to bacterial flagellin is mediated by Toll-like receptor 5. *Nature,* 10(6832), 1099-103.

Hicke, L. (2001). Protein regulation by monoubiquitin. *Nat. Rev. Mol. Cell. Biol.,* 2, 195-201.

Hochstrasser, M., & Kornitzer, D. (1998). In J.M. Peters & J.R. Harris & D. Finley (Eds.), *Ubiquitin and the Biology of the Cell* (pp. 279-302). New York: Plenum.

Huibregtse, J. M., Maki, C. G., & Howley, P. M. (1998). Ubiquitination of the p53 tumor suppressor. In: Peters J-M, Harris JR, Finley D (eds) Ubiquitin and the biology of the cell. Plenum, New York, pp 147-189.

Huibregtse, J. M., Scheffner, M., Beaudenon, S., & Howley, P. M. (1995). A family of proteins structurally and functionally related to the E6-AP ubiquitin-protein ligase. *Proc Natl Acad Sci USA,* 92, 2563-2567.

Kamei, C. L., Boruc, J., Vandepoele, K., Van den Daele, H., Maes, S., et al. (2008). The PRA1 gene family in Arabidopsis. *Plant Physiol,* 147, 1735-1749.

Kawahara, H., & Yokosawa, H. (1992). Cell cycle-dependent change of proteasome distribution during embryonic development of the ascidian *Halocynthia roretzi. Dev. Biol.,* 151, 27-33.

Khorasanizadeh, S., Peters, I. D., Butt, T. R., & Roder, H. (1993). Folding and stability of a tryptophan-containing mutant of ubiquitin. *Biochemistry,* 32, 7054-7063.

Kim, H. S., & Delaney, T. P. (2002). Arabidopsis SON1 is an F-box protein that regulates a novel induced defense response independent of both salicylic acid and systemic acquired resistance. *The Plant Cell,* 14, 1469-1482.

Kraft E, Stone SL, Ma L, Su N, Gao Y, Lau O, Deng X, and Callis J. (2005) Genome Analysis and Functional Characterization of the E2 and RING-Type E3 Ligase Ubiquitination Enzymes of Arabidopsis. *Plant Physiol*., 139:1597-1611.

Lam, E. (2004). Controlled cell death, plant survival and development. *Nat Rev Mol Cell Biol.,* 5, 305-315.

Lecker, S. H., Goldberg, A. L., & Mitch, W. E. (2006). Protein degradation by the ubiquitin-proteasome pathway in normal and disease states. *JASN,* 17(7), 1807-1819.

Lee, D. H., & Goldberg, A. L. (1998). Proteasome inhibitors: valuable new tools for cell biologists. *Trends Cell Biol.,* 8(10), 397-403.

Lenkinski, R. E., Chen, D. M., Glickson, J. D., & Goldstein, G. (1977). Nuclear magnetic resonance studies of the denaturation of ubiquitin. *Biochem. Biophys. Acta,* 494, 126-130.

Liu, L., et al. (2010). An efficient system to detect protein ubiquitination by agroinfiltration in *Nicotiana benthamiana*. *Plant J,* 61, 893-903.

Liu, L., et al. (2012) In vivo ubiquitination assay by agroinfiltration. *Plant Signalling Networks: Methods and Protocols,* 876, 153-162.

Liu H, and Stone SL. (2010). Abscisic Acid Increases *Arabidopsis* ABI5 Transcription Factor Levels by Promoting KEG E3 Ligase Self-Ubiquitination and Proteasomal Degradation. *The Plant Cell*, 22:2630-2641.

Liu, H., & Stone, S. L. (2013). Cytoplasmic degradation of the Arabidopsis transcription factor ABSCISIC ACID INSENSITIVE 5 is mediated by the RING-type E3 ligase KEEP ON GOING. *J. Biol. Chem.,* 288(28), 20267-20279.

Lorick, K. L., Jensen, J. P., Fang, S., Ong, A. M., Hatakeyama, S., & Weissman, A. M. (1999). RING fingers mediate ubiquitin-conjugating enzyme (E2)-dependent ubiquitination. *Proc Natl Acad Sci USA,* 96, 11364-11369.

Lu, D., Lin, W., Gao, W., Wu, S., Cheng, C., et al. (2011). Direct ubiquitination of pattern recognition receptor FLS2 attenuates plant innate immunity. *Science*, 332, 1439-1442.

Lyzenga, W. J., Booth, J. K., & Stone, S. L. (2012). The Arabidopsis RING-type E3 ligase XBAT32 mediates the proteasomal degradation of the ethylene biosynthetic enzyme, 1-aminocyclopropane-1-carboxylate synthase 7. *The Plant Journal,* 71, 23-34.

Metzger, M. B., Pruneda, J. N., Klevit, R. E., & Weissman, A. M. (2014). RING-type E3 ligases: Master manipulators of E2-ubiquitin conjugating enzymes and ubiquitination. *BBA Molecular Cell Research,* 1843(1), 47-60.

Michaelson, L. V. N. (2010). Sphingolipid signaling in plants. In: Munnik T, editor. Lipid signaling in plants, Plant cell monographs. Heidelberg; New York: Springer. Pp. 307-321.

Moon J, Parry G, Estelle M. (2004). The Ubiquitin-Proteasome Pathway and Plant Development. *Plant Cell*; 16(12), 3181-95.

Morel, J. B., & Dangl, J. L. (1997). The hypersensitive response and the induction of cell death in plants. *Cell Death Differ.,* 4, 671-683.

Nodzon, L.A., Xu, W.H., Wang, Y., Pi, L.Y., Chakrabarty, P.K. & Song, W.Y. (2004) The ubiquitin ligase XBAT32 regulates lateral root development in Arabidopsis. *Plant J*., 40(6), 996-1006.

Passmore, L. A., & Barford, D. (2004). Getting into position: the catalytic mechanisms of protein ubiquitylation. *Biochem. J.* 379, 513-525.

Pata, M. O., Hannun, Y. A., Ng, C. K. (2010). Plant sphingolipids: decoding the enigma of the Sphinx. *New Phytol.,* 185, 611-630.

Peng, J., Schwartz, D., Elias, J. E., Thoreen, C. C., Cheng, D., et al. (2003). A proteomics approach to understanding protein ubiquitination. *Nat. Biotechnol.* 21, 921-926.

Pennell LP, and Lamb C. (1997). Programmed cell death in plants. *Plant Cell,* 9, 1157-1168.

Petersen, N. H., Joensen, J., McKinney, L. V., Brodersen, P., Petersen, M., et al. (2009). Identification of proteins interacting with Arabidopsis ACD11. *J Plant Physiol.,* 166, 661-666.

Pickart CM. (2001). Mechanisms underlying ubiquitination. *Annu. Rev. Biochem*.,70: 503-533.

Pickart CM, and Eddins MJ. (2004). Ubiquitin: structures, functions, mechanisms. *Biochem. Biophys. Acta,* 1695, 55-72.

Prasad, M. E., & Stone, S. L. (2010). Further analysis of XBAT32, an Arabidopsis RING E3 ligase, involved in ethylene biosynthesis. *Plant signaling & behavior,* 5, 1425-1429.

Prasad, M. E., Schofield, A., Lyzenga, W., Liu, H., & Stone, S. L. (2010). Arabidopsis RING E3 ligase XBAT32 regulates lateral root production through its role in ethylene biosynthesis. *Plant Physiology*, 153, 1587-1596.

Reape, T. J., & McCabe, P. F. (2008). Apoptotic-like programmed cell death in plants. *New Phytol.,* 180, 13-26.

Ronald, P. C., Albano, B., Tabien, R., Abenes, L., Wu, K. S., McCouch, S., & Tanksley, S. D. (1992). Genetic and physical analysis of the rice bacterial blight disease resistance locus, Xa21. *Mol Gen Genet.,* 236, 113-120.

Sadanandom, A., Bailey, M., Ewan, R., Lee, J., & Nelis, S. (2012). The ubiquitin-proteasome system, central modifier of plant signaling. *New Phytol.,* 196, 13-28.

Sadowski, M., Suryadinata, R., Tan, A. R., Roesley, S. N. A., & Sarcevic, B. (2012). Protein monoubiquitination and polyubiquitination generate structural diversity to control distinct biological processes. *Life,* 64(2), 136-142.

Schnell, J. D., Hicke, L. (2003). Non-traditional functions of ubiquitin and ubiquitin-binding proteins. *J Biol Chem,* 278, 35857-35860.

Sedgwick SG, and Smerdon SJ. (1999). The Ankyrin Repeat: A Diversity of Interactions on a Common Structural Framework. *Trends Biochem. Sci*., 24:311-6.

Seemuller, E., Lupas, A., Stock, D., Lowe, J., Huber, R., & Baumeister, W. (1995). Proteasome from *Thermoplasma acidophilum*: a threonine protease. *Science,* 268(5210), 579-582.

Shirasu, K., & Schulze-Lefert, P. (2000). Regulators of cell death in disease resistance. *Plant Mol Biol.,* 44, 371-385.

Simanshu, D. K., Zhai, X., Munch, D., Hofius, D., Markham, J. E., Bielawski, J., Bielawska, A., … & Brown, R. E. (2014). Arabidopsis accelerated cell death 11, ACD11, is a ceramide-1-phosphate transfer protein and intermediary regulator of phytoceramide levels. *Cell Rep.,* 6(2), 388-399.

Smalle J, and Vierstra RD. (2004). The Ubiquitin 26S Proteasome Proteolytic Pathway. Annual Review of Plant Biology; 55(1):555-90.

Song, W. Y., Wang, G. L., Chen, L. L., Kim, H. S., Pi, L. Y., et al. (1995). A receptor kinase-like protein encoded by the rice disease resistance gene, Xa21. *Science,* 270, 1804-1806.

Sparkes, I. A., Runions, J., Kearns, A., Hawes, C. (2006). Rapid, transient expression of fluorescent fusion proteins in tobacco plants and generation of stably transformed plants. *Nat Protoc.,* 1, 2019-2025.

Stone, S. L. (2014). The role of ubiquitin and the 26S proteasome in plant abiotic stress signaling. *Front Plant Sci.,* 5, 135.

Stone SL, and Callis J. (2007). Ubiquitin ligases mediate growth and development by promoting protein death, *Curr. Opin. Plant Biol,* 10, 624-632.

Stone SL, Hauksdottir H, Troy A, Herschleb J, Kraft E, and Callis J. (2005). Functional Analysis of the Ring-Type Ubiquitin Ligase Family of Arabidopsis. *Plant Physiol*., 137: 13-30.

Stone SL, Williams LA, Farmer LM, Vierstra RD, and Callis J (2006). KEEP ON GOING, a RING E3 ligase Essential for Arabidopsis Growth and Development, is Involved in Abscisic Acid Signaling. *Plant Cell*, 18:3415-3428.

Sun L, and Chen ZJ (2004). The Novel Functions of Ubiquitination in Signaling. *Curr. Opin. Cell Biol.,*16: 119-126.

Takahashi, Y., Berberich, T., Kanzaki, H., Matsumura, H., Saitoh, H., Kusano, T., & Terauchi, R. (2009). Unraveling the roles of sphingolipids in plant innate immunity. *Plant Signal Behav.,* 4(6), 536-538.

Turner, J. G., Ellis, C., & Devoto, A. (2002). The jasmonate signal pathway. *The Plant Cell,* 14, 153-164.

Van den Burg, H. A., Tsitsigiannis, D. I., Rowland, O., Lo, J., Rallapalli, G., Maclean, D., … & Jones, J. D. (2008). The F-box protein ACRE189/ACIF1 regulates cell death and defense responses activated during pathogen recognition in tobacco and tomato. *The Plant Cell*, 20, 697-719.

Verdecia, M. A., Joazeiro, C. A. P., Wells, N. J., Ferrer, J. L., Bowman, M. E., Hunter, T., & Noel, N. P. (2003). Conformational flexibility underlies ubiquitin ligation mediated by the WWP1 HECT domain E3 ligase. *Molecular Cell,* 11(1), 249-259.

Vierstra, R. D. (2009). The ubiquitin-26S proteasome system at the nexus of plant biology. *Nat Rev Mol Cell Biol.,* 10(6), 385-397.

Voges, D., Zwickl, P., & Baumeister, W. (1999). The 26S proteasome: A molecular machine designed for controlled proteolysis. *Annu. Rev. Biochem.,* 68, 1015-1068.

Wang, Y. S., Pi, L. Y., Chen, X., Chakrabarty, P. K., Jiang, J., et al. (2006). Rice XA21 binding protein 3 is a ubiquitin ligase required for full Xa21-mediated disease resistance. *The Plant Cell,* 18, 3635-3646.

Wang, F., Zhu, D., Huang, X., Li, S., Gong, Y., Yao, Q., … & Deng, X. W. (2009). Biochemical insights on degradation of *Arabidopsis* DELLA proteins gained from a cell-free assay system. *Plant Cell,* 21, 2378-2390.

Weissman, A. M. (2001). Themes and variations on ubiquitylation. *Nat Rev Mol Cell Biol,* 2, 169-178.

Wenzel, T., Eckerskorn, C., Lottspeich, F., & Baumeister, W. (1994). Existence of a molecular ruler in proteasomes suggested by analysis of degradation products. *FEBS Lett.,* 349(2), 205-209.

Wu, G., Xu, G., Schulman, B. A., Jeffrey, P. D., Harper, J. W., et al. (2003). Structure of a beta-TrCP1-Skp-1-beta-catenin complex: destruction motif binding and lysine specificity of the SCF(beta-TrCP1) ubiquitin ligase. *Mol. Cell,* 11, 1445-1456.

Yuan X, Zhang S, Liu S, Yu M, Su H, et al. (2013) Global analysis of ankyrin repeat domain C3HC4-type RING finger gene family in plants. *PLoS One,* 8(3), e58003.

Zheng, N., Wang, P., Jeffrey, P. D., & Pavletich, N. P. (2000). Structure of a c-Cbl-UbcH7 complex RING domain function in ubiquitin-protein ligases. *Cell,* 102, 533-539.

Zipfel, C., Robatzek, S., Navarro, L., Oakeley, E. J., Jones, J. D., Felix, G., & Boller, T. (2004). Bacterial disease resistance in Arabidopsis through flagellin perception. *Nature,* 428, 764-767.